

12-14-2006

# Coulomb oscillation in the hydrogen atom and molecule ion

Manfred Bucher

Physics Department, California State University, Fresno  
Fresno, California 93740-8031

## Abstract

Semiclassical oscillation of the electron through the nucleus of the  $H$  atom yields both the exact energy and the correct orbital angular momentum for  $l = 0$  quantum states. Similarly, electron oscillation through the nuclei of  $H_2^+$  accounts for a stable molecule ion with energy close to the quantum mechanical solution. The small discrepancy arises from the neglect of the electron's wave nature.

PACS numbers: 03.65.Sq, 31.10.+z, 31.20.Pv

## I. INTRODUCTION

Two of the reasons why the old quantum theory of Bohr and Sommerfeld was abandoned in the mid 1920s were the theory’s failure to give the correct multiplet structure of the hydrogen atom and the stability of the hydrogen molecule ion,  $H_2^+$ .<sup>1</sup> The old vector model of angular momentum<sup>2</sup> gave, for a given principal quantum number  $n$ , sublevels with angular quantum numbers  $l = 1, 2, \dots, n$ .<sup>3</sup> Spectroscopic evidence, however, showed multiplicities of spectral line splitting in a magnetic field according to  $l = 0, 1, \dots, n - 1$ . Max Jammer, in his review,<sup>2</sup> notes that “the old quantum theory could never resolve this inconsistency.”

A treatment of the hydrogen molecule ion with Sommerfeld’s quantization conditions had been Wolfgang Pauli’s doctoral thesis of 1922.<sup>4</sup> Pauli found its molecular binding energy to be positive (non-binding)—contrary to (later) experimental findings. Martin Gutzwiller<sup>5</sup> thinks that “the solution of this problem can be rated, with only slight exaggeration, as the most important in quantum mechanics, because if an energy level with a [more] negative value [than of a free hydrogen atom] can be found, then the chemical bond between two protons by a single electron has been explained.”

Both dilemmas of the old quantum theory can be resolved, though, with a single extension: an oscillation of the electron through the nucleus (nuclei) of the atom (molecule). In essence this solution is already formally included in Sommerfeld’s theory of the hydrogen atom<sup>6</sup> but was explicitly omitted by Sommerfeld and his school as being *unphysical*. The case in point, obtained with Sommerfeld’s quantization conditions for radial and angular motion, is a quantum state with zero angular action, characterized by an angular quantum number  $l = 0$ . What is its orbit?

The geometry of an  $nl$  Sommerfeld ellipse is given by its semimajor axis,  $a_{nl} = (r_B/Z)n^2$ , and semiminor axis,  $b_{nl} = (r_B/Z)n\sqrt{l(l+1)}$ .<sup>7</sup> Here  $r_B = h^2/4\pi^2me^2$  is the Bohr radius in terms of fundamental constants, serving as an atomic distance unit, and  $Ze$  is the nuclear charge. An  $(n, 0)$  orbit is thus a line ellipse with its nuclear focus at one end and its empty focus at the other. This case was regarded as unphysical because of the electron’s collision with the nucleus—an uncritical adaptation from celestial mechanics. A closer inspection confirms that a line ellipse with *terminal* nuclear focus is indeed unphysical—but for quite a different reason!

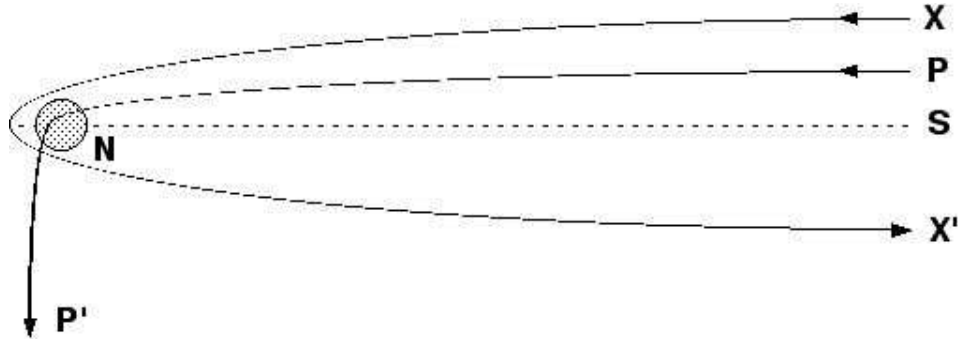


Fig. 1. Partial trajectory of an extranuclear orbit  $XX'$  and of a penetrating orbit  $PP'$  through nucleus  $N$ . The dotted line  $S$  shows the major symmetry axis of  $XX'$ .

Leaving quantization conditions momentarily aside, what would happen if we *continuously* decrease an angular quantum number  $\lambda$  while keeping the principal quantum number  $n$  constant? We then would get more and more slender ellipses with the same length of major axis,  $2a_n$ . By basic electric theory, the nuclear Coulomb potential outside a *finite-size* nucleus  $N$  is given by the point potential as if all nuclear charge,  $+Ze$ , was concentrated at the center of the nucleus. This holds as long as the electron orbit stays outside the nucleus. Two borderline cases are illustrated in Fig. 1. For a very small  $\lambda$  value, say  $0 < \lambda_X \ll 1$ , we obtain a very slender elliptical orbit with partial trajectory  $XX'$  about the nucleus. Further decrease of  $\lambda$  to  $\lambda_P < \lambda_X$  causes an intrusion of the electron into the finite nucleus of radius  $r_N$  (see trajectory  $PN$  in Fig. 1). Once inside, at a distance  $r < r_N$  from the center, then, by Gauss's law, only a fraction of the nuclear charge,  $Z'(r)e < Ze$ , acts on the electron via centripetal force.<sup>8</sup> Accordingly, the electron's exit trajectory  $NP'$  is no longer symmetric to its approach trajectory  $PN$  with respect to the major axis  $S$  of the (partial) ellipse  $XX'$ . In the extreme case of a head-on penetration of the nucleus,  $\lambda = 0$ , there is no centripetal force at all! The electron will then, with almost constant speed, traverse the nucleus, continue, with decreasing speed, to the opposite turning point of its line orbit and revert its motion periodically. We want to call the electron's straight-line oscillation in the Coulomb potential of a finite-size nucleus a "*Coulomb oscillator*."

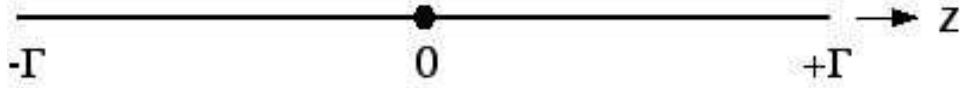


Fig. 2. Line orbit of a Coulomb oscillator with nucleus at origin 0 and turning points at  $\pm\Gamma$ .

## II. HYDROGEN ATOM

For the formal treatment of the non-relativistic Coulomb oscillator we designate the  $z$  axis along the line orbit, with turning points at  $z = \pm\Gamma$  and nuclear position at  $z = 0$  (see Fig. 2). The electron's total energy  $E$  at position  $z$  must equal the potential energy at a turning point,

$$E = \frac{1}{2}mv^2 - \frac{Ze^2}{|z|} = -\frac{Ze^2}{\Gamma}. \quad (1)$$

This gives the electron's speed along the  $z$  axis,

$$v = \pm e\sqrt{\frac{2Z}{m}}\sqrt{\frac{1}{|z|} - \frac{1}{\Gamma}}. \quad (2)$$

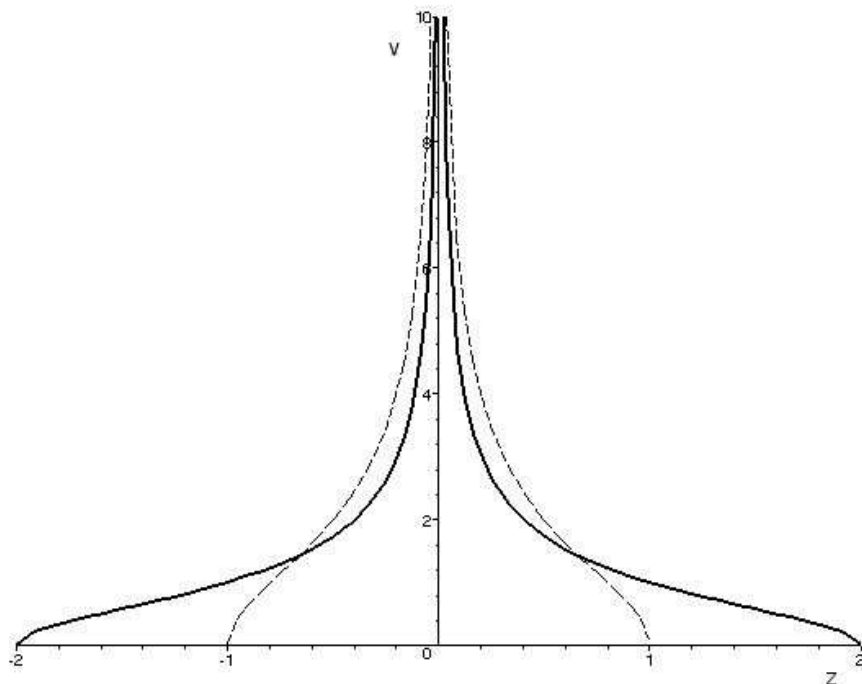


Fig. 3. Axial electron speed  $v$  vs. position  $z$  of an electron in Coulomb oscillation for the ground state,  $n = 1$ , of a hydrogen atom  $H$  ( $Z = 1$ , solid curve) and a helium ion  $He^+$  ( $Z = 2$ , dashed curve). The area under one wing of each curve represents the radial action,  $A = 1h$ .

Figure 3 displays its dependence on the axial position as a two-wing curve cusped at the nucleus. Atomic units (*a.u.*) are used, that is, the Bohr radius  $r_B$  and the “Bohr speed”  $v_B = 2\pi e^2/h = \alpha c$ —the electron speed in the ground-state Bohr orbit of the  $H$  atom—with fine-structure constant  $\alpha \approx 1/137$  and speed of light  $c$ . The curve’s wing along the positive  $z$  axis,  $|z| = r$ , gives the *radial* speed,  $v_r(r) = |v(z)|$ , necessary for Sommerfeld’s *radial* quantization condition,

$$\oint p_r dr = m \oint v_r(r) dr = n_r h. \quad (3)$$

Here  $p_r$  is the radial momentum,  $n_r = 1, 2, \dots$  is the radial quantum number, and  $h$  is Planck’s quantum of action. Integration is over one period of the

radial motion,  $z = +\Gamma \rightarrow 0 \rightarrow +\Gamma$ . Graphically, the radial quantization is illustrated in Fig. 3 by the area under *one* wing of the speed curve. For a line orbit,  $l = 0$ , the radial quantum number equals the principal quantum number,  $n \equiv n_r + l = n_r$ .

In order to express the radial quantization in terms of *axial* motion we employ a “fold-out factor,”  $\phi = 2$ , to compensate for the doubling of integration range in the extension from the radial one-wing speed curve to the axial two-wing curve. The quantization is thus restated,

$$\frac{1}{\phi} \oint p_z dz = \frac{m}{\phi} \oint v(z) dz = n_z h, \quad (3')$$

with axial quantum number  $n_z = n_r = n$  and integration over the axial double-wing range,  $z = +\Gamma \rightarrow -\Gamma \rightarrow +\Gamma$ . By symmetry we can restrict the axial action integral to one quarter of the oscillation, say  $z = +\Gamma \rightarrow 0$ ,

$$\frac{1}{\phi} \oint p_z dz = -\frac{4m}{\phi} \int_{\Gamma}^0 v(z) dz = -\frac{4e}{\phi} \sqrt{2Zm} \int_{\Gamma}^0 \sqrt{\frac{1}{z} - \frac{1}{\Gamma}} dz = nh. \quad (4)$$

Here the electron’s motion in the negative  $z$  direction is accounted for by the negative sign. Although the electron’s speed through a point nucleus diverges,  $v(0) = \infty$ , the action integral, Eq. (4), stays finite and determines the quantized amplitude  $\Gamma_n$  of the Coulomb oscillator. Graphically the amplitude  $\Gamma_n$  must be such that it stretches the speed curve horizontally to the extent that the area under one wing,  $A_n = nh$ , represents the quantized action. The analytic solution, derived in Appendix A, is

$$\Gamma_n = 2 \frac{r_B}{Z} n^2. \quad (5)$$

Inserting Eq. (5) into Eq. (1) yields the quantized energy,

$$E_n = -\frac{Z^2 e^2}{\Gamma_n} = -\frac{Z^2}{n^2} R_y, \quad (6)$$

in terms of the Rydberg energy unit,  $R_y = 2\pi^2 m e^4 / h^2 = 13.6 \text{ eV}$ , and in agreement with the energy of the  $n$ th Bohr orbit.

Note that Eq. (5) gives the amplitude of the  $n$ th Coulomb oscillator as *twice* the radius of the  $n$ th Bohr orbit or of the semimajor axis of an

$nl$  Sommerfeld ellipse,  $r_n = a_{nl} = (r_B/Z)n^2$ . For comparison, the time-average radial distance of a Kepler orbit<sup>9</sup> of major and minor semiaxes  $a$  and  $b$ , respectively, is  $\langle r \rangle_t = (3a^2 - b^2)/(2a)$ . A line ellipse ( $b = 0$ ) has then  $\langle r \rangle_t = \frac{3}{2}a$ . Applied to an  $nl$  Sommerfeld orbit,<sup>9</sup> its average size,  $\langle r_{nl} \rangle_t = (r_B/Z)[3n^2 - l(l + 1)]/2$ , is in agreement with the corresponding quantity from quantum mechanics,<sup>10</sup>  $\langle r_{nl} \rangle = \int \psi^* r \psi d^3r$ . Thus the time-average radial distance of a Coulomb oscillator is  $\langle r_{n0} \rangle_t = \frac{3}{2}(r_B/Z)n^2$ . For the ground state of the hydrogen atom,  $n = 1$ , this gives  $\langle r_{10} \rangle_t = \frac{3}{2}r_B$ , as is well-known from quantum mechanics.<sup>10</sup>

The concept of the electron's semiclassical Coulomb oscillation is consistent with the Fermi-contact term of hyperfine interaction for  $l = 0$  states, which arises from the presence of the electron *inside* the nucleus. This is familiar from quantum mechanics<sup>11</sup> and can be interpreted semiclassically as a local-field effect.<sup>12</sup>

To be sure, the extension of Sommerfeld's theory by the Coulomb oscillator resolves the discrepancy of the old quantum theory with spectroscopy, mentioned above, only at the *low* end of angular quantum numbers,  $l = 0$ . The resolution at the high end—repeal of the circular Bohr orbit,  $l \neq n$ —involves an analysis in terms of space quantization which is beyond the scope of the present study.

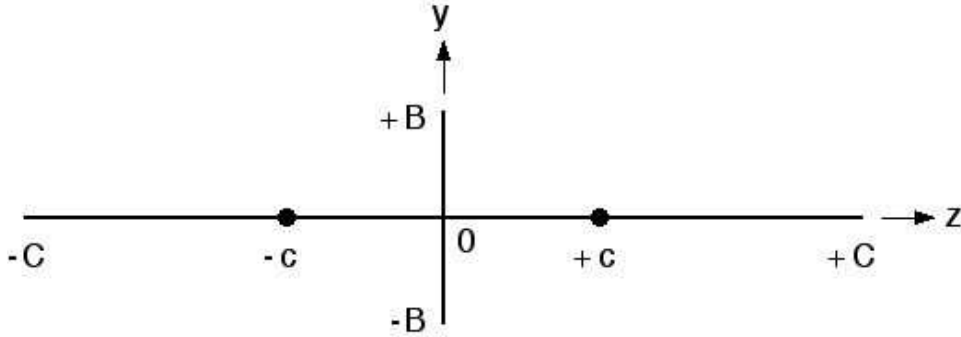


Fig. 4. Axial Coulomb oscillation in an  $H_2^+$  molecule ion between axial turning points  $\pm C$  and through nuclei at  $\pm c$ ; perpendicular oscillation between lateral turning points  $\pm B$  and through midpoint 0.

### III. HYDROGEN MOLECULE ION

#### A. Formalism

A hydrogen molecule ion,  $H_2^+$ , consists of two proton nuclei and one electron. We assume, in adiabatic approximation, the protons located at fixed positions  $z = \pm c$  on the molecular axis (see Fig. 4). The term ‘‘Coulomb oscillator’’ denominates again the motion of a point electron, now along either the line through the protons ( $z$  axis) and with turning points  $\pm C$ , or along the perpendicular line through the midpoint ( $y$  axis) with turning points  $\pm B$ . The molecule ion’s total energy  $E$  at any position on the axis,  $-C \leq z \leq +C$ , must equal the potential energy at the turning point  $C$ ,

$$E = \frac{1}{2}mv^2 - \frac{e^2}{|z+c|} - \frac{e^2}{|z-c|} + \frac{e^2}{2c} = -\frac{e^2}{C+c} - \frac{e^2}{C-c} + \frac{e^2}{2c}. \quad (7)$$

For electron positions beyond the protons,  $z > c$ , this gives an electron speed

$$v_{out} = \pm \frac{2e}{\sqrt{m}} \sqrt{\frac{z}{z^2 - c^2} - \frac{C}{C^2 - c^2}}. \quad (8a)$$

For positions between the protons,  $0 < z < c$ , the corresponding speed is

$$v_{in} = \pm \frac{2e}{\sqrt{m}} \sqrt{\frac{c}{c^2 - z^2} - \frac{C}{C^2 - c^2}}. \quad (8b)$$

The speed expressions will be used in the action integral,

$$\frac{1}{\phi} \oint p_z dz = \frac{2m}{\phi} \int_C^{-C} v(z) dz = A_z = A_{out} + A_{in}, \quad (9)$$

with outer contribution

$$A_{out} = \frac{2m}{\phi} \left[ \int_C^c v_{out}(z) dz + \int_{-c}^{-C} v_{out}(z) dz \right] \quad (10a)$$

and inner contribution

$$A_{in} = \frac{2m}{\phi} \int_c^{-c} v_{in}(z) dz. \quad (10b)$$



Here  $\phi$  is a fold-out factor to be specified below.

If the conditions are such that the electron swings along the  $z$  axis through the midpoint 0, that is,  $v_{in}(0) > 0$ , then there exists also an oscillation along the  $y$  axis with lateral speed  $u$ , having the same total energy,

$$E = \frac{1}{2}mu^2 - \frac{2e^2}{\sqrt{y^2 + c^2}} + \frac{e^2}{2c} = -\frac{2e^2}{\sqrt{B^2 + c^2}} + \frac{e^2}{2c}. \quad (11)$$

Equal energy at the axial and lateral turning points,  $E(C) = E(B)$ , Eqs. (7) and (11), determines the latter's geometric dependence,

$$B = \sqrt{C^2 + \frac{c^4}{C^2} - 3c^2}. \quad (12)$$

Solving Eq. (11) for the lateral speed,

$$u = \pm \frac{2e}{\sqrt{m}} \sqrt{\frac{1}{\sqrt{y^2 + c^2}} - \frac{1}{\sqrt{B^2 + c^2}}}, \quad (13)$$

provides the integrand of the action integral over a lateral oscillation,

$$A_y = \frac{1}{\phi} \oint p_y dy = \frac{2m}{\phi} \int_B^{-B} u(y) dy. \quad (14)$$

Subtraction of the protons' mutual repulsion from the total energy  $E$  of axial or lateral motion, Eqs. (7) and (11), gives the *electronic* energy,

$$E_{el} = E - \frac{e^2}{R}, \quad (15)$$

in its dependence on the proton separation,  $R = 2c$ . This brackets the molecular problem with known atomic results, Eq. (6), in the limits of  $R = \infty$  (free  $H$  atom,  $Z = 1$ ) and  $R = 0$  (free  $He^+$  ion,  $Z = 2$ ). For those cases, as well as any proton-proton distance  $R$  between, we keep the action constant,

$$A = A_z + A_y = nh. \quad (16)$$

Equation (16) is the *Einstein* quantization condition<sup>13</sup>—a generalization of Sommerfeld's quantization over separable variables—where the *quantum sum* equals the sum of action integrals over topologically independent paths in phase space.<sup>14</sup>

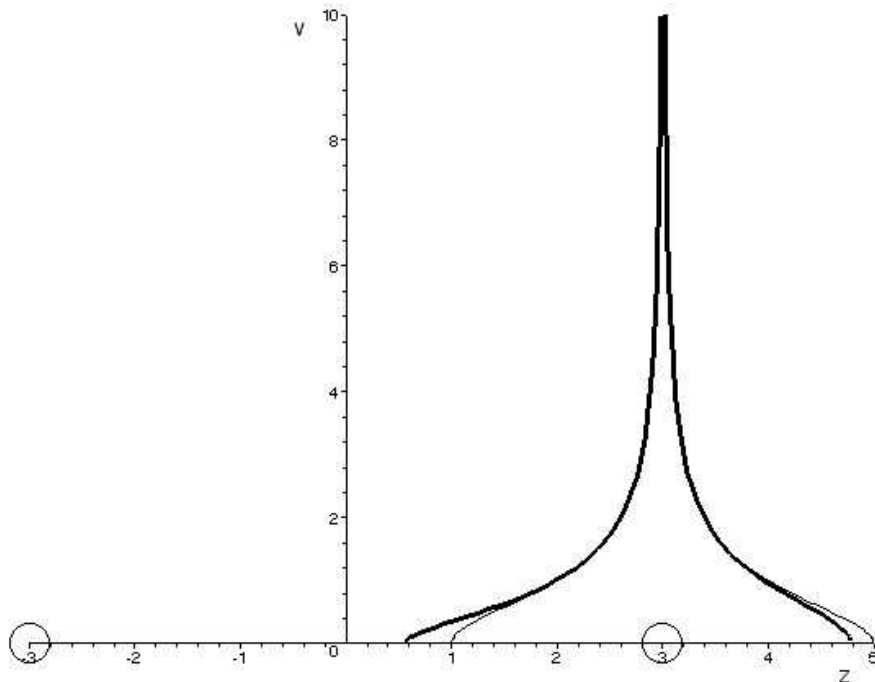


Fig. 5. Axial speed  $v$  vs. position  $z$  in the ground state of an  $H_2^+$  molecule ion (bold curve) and, for comparison, of a free  $H$  atom (thin curve). Circles indicate the axial the positions of the nuclei, here with a *large* separation,  $R = 6 r_B$ .

Here we treat the molecule ion only in its *ground state*,  $n = 1$ . Analytic solutions of the action integrals, Eqs. (10ab) and (14), are complicated due to elliptic functions. We therefore integrate numerically and visualize the integrals by the area under the corresponding speed curves. The bold curve in Fig. 5 shows the axial electron speed  $v(z)$  for a *far* proton separation,  $R = 6 r_B$ . The electron, in its semiclassical motion, then oscillates only about (and through) the right proton. The area under the speed curve, Eq. (8ab), proportionally represents the ground state's unity of action,  $m \oint v(z) dz = \phi h$ , with a fold-out factor  $\phi = 2$  in analogy to the free-atom case, Eq. (4). The thin curve shows, for comparison, the axial electron speed in a free  $H$  atom—familiar from Fig. 3—centered at the same proton position,  $+c$ . The pull from the left proton (at  $-c$ ) on the oscillating electron can be seen by the

distortion of the speed function  $v(z)$  and the redistribution of the area under the curve.

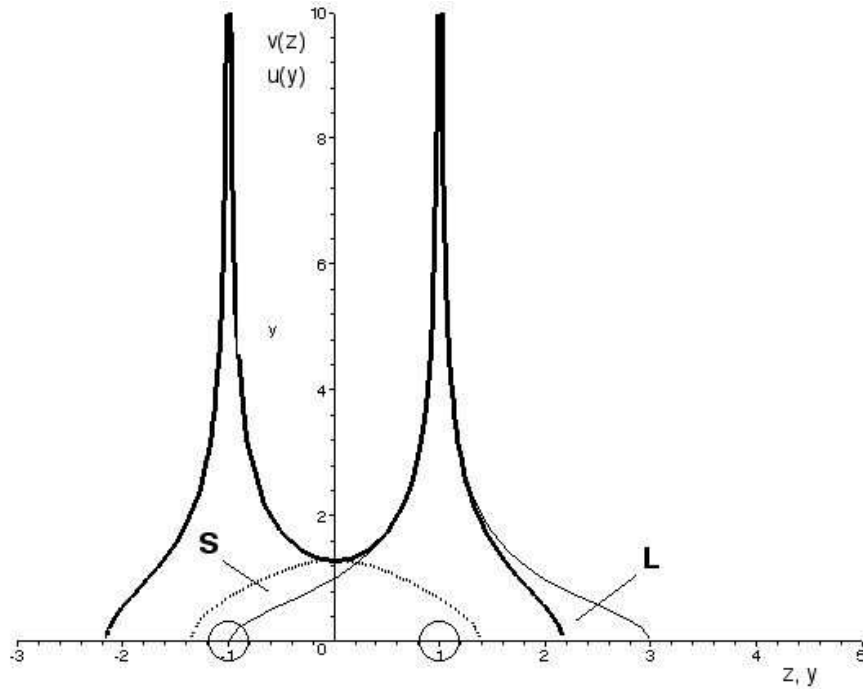


Fig. 6. Axial speed  $v$  vs. position  $z$  in the ground state of an  $H_2^+$  molecule ion (M-shaped bold curve) and, for comparison, of a free H atom ( $\Lambda$ -shaped thin curve, centered at the right nucleus). The  $\cap$ -shaped dotted curve, centered at 0, shows the lateral speed  $u$  vs. the perpendicular position  $y$  in the molecule. Circles indicate the axial positions of the nuclei, here with a *small* separation,  $R = 2 r_B$ .

When, with closer proton separation  $R$ , as in Fig. 6, the electron swings past the midpoint 0, then the single-cusp speed curve  $v(z)$  from Fig. 5—akin in shape to letter  $\Lambda$ —becomes double-cusped (akin to letter M) and symmetric with respect to the bisector ( $y$  axis). Now there is also a lateral oscillation with speed  $u(y)$  having the same total energy  $E$ . The equality of  $E$  in both cases can be seen in Fig. 6 by the equality of axial and lateral speed

at the midpoint,  $v(0) = u(0)$ —a position where the electron experiences the same potential in either case. For convenience the lateral speed  $u(y)$ , though perpendicular to the proton axis, is displayed in Fig. 6 together with the axial speed  $v(z)$ . The lateral speed curve  $u(y)$ , drawn dotted, is readily recognized by its dome shape ( $\cap$ ). At the bifurcation value of the proton separation,  $\check{R}$ , where the electron starts swinging through the midpoint 0, the axial speed curve  $v(z)$  changes from its one-centered  $\Lambda$  shape to a two-centered M shape. The *area* under the axial speed curve then abruptly doubles,  $M(\check{R} - \delta) \approx 2\Lambda(\check{R} + \delta)$ , upon a very small change in proton separation,  $\delta \ll \check{R}$ . In order to keep the action integral continuous at  $\check{R}$ , the sudden area doubling is compensated by a corresponding doubling of the fold-out factor from  $\phi = 2$  for  $R > \check{R}$  to  $\phi = 4$  for  $R < \check{R}$ . The same fold-out factor,  $\phi = 4$ , must be used for the lateral action integral  $A_y$ , Eq. (14), as will become clear shortly.

The unity of action,  $A = 1h$ , is visualized again in Fig. 6. To this end we compare the right half of the bold M-shape curve of axial electron speed in the molecule with the thin curve  $\Lambda(H)$  of the axial speed in a free  $H$  atom positioned at the right nucleus,  $+c$ . Due to attraction from the left nucleus, the right wing of the M curve is smaller than that of  $\Lambda(H)$  by the area of lobe  $L$ . On the other hand, the left flank of the  $\Lambda(H)$  curve that extends over the negative  $z$  axis is smaller than the left wing of the lateral speed curve  $\cap$  by the area of slice  $S$ . The area under the free-atom curve is then

$$\Lambda(H) \approx \frac{1}{2}M + L + \frac{1}{2}\cap - S. \quad (17a)$$

The areas of lobe and slice are comparable,

$$L \approx S. \quad (17b)$$

When the tiny notch to the right of the saddle point of M is taken into account, then the approximations (17ab) become equations and combine to

$$M + \cap = 2\Lambda(H). \quad (18)$$

The area under both the axial and lateral speed curves is thus four times the area under *one* wing of the free-atom curve,  $M + \cap = 4 \times \frac{1}{2}\Lambda(H)$ . Since the latter represents one quantum of action,  $h$ , the combined area  $M + \cap$  visualizes its *double* fold-out,  $\phi = 4$ .

With very close proximity of the nuclei,  $R \rightarrow 0$ , the crests of the M curve start merging while its saddle point,  $v(0)$ , keeps rising. In the  $R = 0$  limit of

fusing nuclei the axial electron speed becomes that of a free  $He^+$  ion,  $M \rightarrow \Lambda(He^+)$ , familiar from Fig. 3. Concurrently, the lateral speed curve  $\cap$  rises at its peak,  $u(0) = v(0)$ , and narrows at its base until it, too, turns into the speed curve of the free  $He^+$  ion,  $\cap \rightarrow \Lambda(He^+)$ . In the  $R = 0$  limit the three curves merge,  $M(0) = \cap(0) = \Lambda(He^+)$ .

The results of the Coulomb-oscillator approach will be compared with another semiclassical calculation of  $H_2^+$ , by Strand and Reinhardt.<sup>15</sup> These authors, like Pauli,<sup>4</sup> separate the equation of motion in spheroidal coordinates,  $\xi = (r_+ + r_-)/2c$ ,  $\eta = (r_+ - r_-)/2c$  and  $\varphi$  by virtue of the constants of the motion: total energy  $E$ , angular momentum  $\mathbf{M}$  about the  $z$  axis, and a component of the bifocal Runge-Lenz vector,  $\Omega_c$ .<sup>16</sup> Here  $r_+$  ( $r_-$ ) is the distance of the electron from the nucleus at  $+c$  ( $-c$ ). Strand and Reinhardt (SR) solve the ensuing one-dimensional differential equations with classical Poisson-bracket techniques. They find the electron's trajectories conditionally periodic<sup>17</sup> and regionally confined due to restrictions from  $E$ ,  $\mathbf{M}$  and  $\Omega_c$ . However, unlike Pauli, who used Sommerfeld quantization, SR employ the Einstein-Brillouin-Keller (EBK) quantization conditions,

$$A_j = \oint p_j dj = (n_j + \frac{1}{2})h, \quad j = \xi, \eta \quad (19ab)$$

and

$$A_\varphi = \oint p_\varphi d\varphi = n_\varphi h. \quad (19c)$$

The background of EBK quantization touches on the foundations of classical and quantum mechanics.<sup>18</sup> For the present purpose its essential rationale may be summarized as follows: A semiclassical treatment involves turning points of radial, or other librating motion. Any tunneling through “forbidden” regions of negative kinetic energy is ruled out. Viewed in terms of the quantum mechanical WKB (Wentzel-Kramers-Brillouin) approximation, the hard reflection of a wavefunction at a turning point corresponds to a so-called “loss” of phase (phase shift by  $\pi$ ) compared to the soft reflection caused by tunneling (phase shift by  $\pi/2$ ). This shortcoming can be remedied with EBK quantization conditions by addition of a value of  $1/4$ , for each librational turning point, to the corresponding quantum number. Such is the case for the electron's elliptical and hyperbolic librations in the above quantization, Eq. (19ab), but not for a rotation about the  $z$  axis, Eq. (19c). Strand

and Reinhardt call these quantization conditions “primitive” to distinguish them from more sophisticated ones, specified below.

A semiclassical treatment of a free  $H$  atom with EBK quantization has recently been presented in these pages.<sup>19</sup> In this case the isotropic symmetry permits a separation of variables in spherical coordinates,  $r$ ,  $\theta$  and  $\varphi$ , and the EBK quantization conditions are like Eqs. (19abc) except for  $j = r, \theta$ . The atomic ground state is characterized by the quantum numbers  $(n_r, n_\theta, n_\varphi) = (0, 0, 0)$ . Accordingly, the action in the atom’s ground state,  $A_1 = 1h$ , is attributed only to tunneling at the radial and latitudinal turning points (the former being the nucleus). Applying EBK quantization to the ground state of  $H_2^+$ , denoted  $1s\Sigma_g$  in molecular spectroscopy, SR likewise assign the quantum numbers  $(n_\xi, n_\eta, n_\varphi) = (0, 0, 0)$ .

## B. Results

Energies of the Coulomb oscillator (CO), in adiabatic dependence on the proton separation, are listed in Appendix B and shown in Fig. 7 in comparison with exact quantum mechanical (QM) results and the semiclassical calculation by SR.<sup>15</sup> The lower part of Fig. 7 shows the electronic energy  $E_{el}(R)$  of the ground state,  $1s\Sigma_g$ . At *large* proton separations,  $R > 6 r_B$ , both the SR calculation (circles) and the CO approach (crosses) agree excellently with the exact QM values (curve). This is the situation where the electron stays near one nucleus (see Fig. 5). As Fig. 7 further shows, such agreement ceases once the classical electron motion leads beyond the molecular bisector, which happens for proton separations below the bifurcation value,  $R < \tilde{R} \approx 5.57 r_B$  (see Fig. 6). Interestingly, the deviations of CO and SR from QM are opposite over the entire range. The SR results are *discontinuous* at a certain proton separation,  $R^* \approx 1.38 r_B$ . Remarkably, at (or near) that value,  $R^*$ , the CO energy crosses the curve of the QM solution.

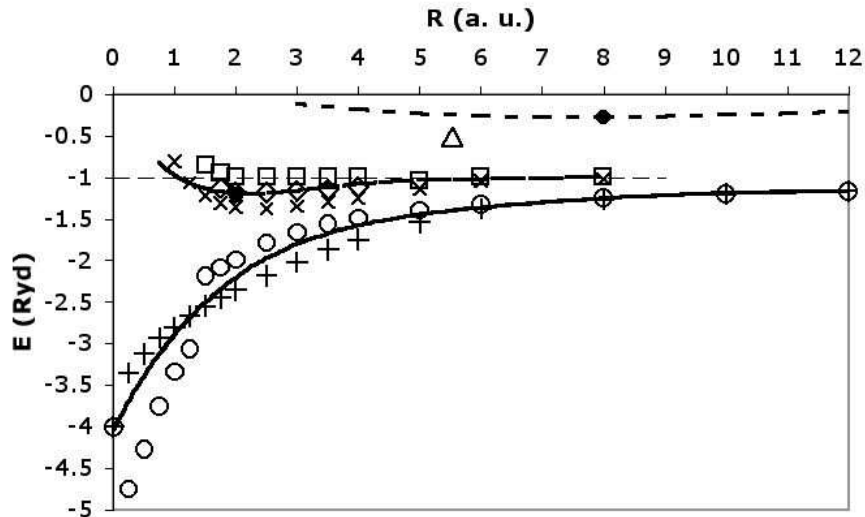


Fig. 7. Dependence of energies of  $H_2^+$  on internuclear distance  $R$ .

*Bottom:* Electronic energy  $E_{el}$  from quantum mechanics (QM, solid curve), primitive semiclassical quantization by Strand and Reinhardt (SR,  $\circ$ ) and the present Coulomb-oscillator approach (CO,  $+$ ).

*Middle:* Total energy  $E$  of the  $1s\Sigma_g$  ground state from QM (dashed curve) with minimum ( $\bullet$ ), values by SR ( $\square$ ) and CO ( $\times$ ) and their average ( $\diamond$ ), energy of a free  $H$  atom (dashed horizontal line).

*Top:* Total energy  $E$  of the  $2p\Pi_u$  state from QM (dotted curve) with minimum ( $\bullet$ ), and historical value by Pauli and Niessen ( $\triangle$ ).

Adding to the electronic energy  $E_{el}$  the proton-proton repulsion gives the *total* energy  $E$ , Eq. (15). The middle part of Fig. 7 shows by the dashed curve the exact total energy  $E(R)$  of the  $1s\Sigma_g$  ground state, obtained from QM and, by symbols, the corresponding CO and SR values. The solid dot at the minimum of the curve shows the QM equilibrium energy, in agreement with experiment,  $E_0 = -1.20 R_y$ , and the equilibrium internuclear distance,

$R_0 = 2.00 r_B$ . The CO energy ( $\times$ ) comes out too low, due to the inaccuracy of its  $E_{el}$ , with an equilibrium value  $E_0(CO) \approx -1.38 R_y$  at  $R_0(CO) \approx 2.5 r_B$ . Conversely, the SR energy ( $\square$ ) comes out too high with  $E_0(SR) \approx -1.05 R_y$  at  $R_0(SR) \approx 5 r_B$ . Since the CO and SR results deviate about equal and oppositely from QM, their *average* ( $\diamond$ ) is close to the exact values with a minimum of  $E_0[\frac{1}{2}(CO + SR)] \approx -1.19 R_y$  at  $R_0[\frac{1}{2}(CO + SR)] \approx 2.5 r_B$ .

The molecular binding energy is the difference of  $E$  in the molecule and in the constituting atoms, here,  $E_0(H_2^+) - E(H)$ . The energy of a free hydrogen atom,  $E(H) = -1 R_y$ , is indicated in Fig. 7 by the fine horizontal line. Both semiclassical treatments, CO and (barely) SR, yield molecular binding energies with *negative* values and thus a *stable* molecule ion. Why are they more successful than the early attempts, in the 1920s, by Pauli,<sup>4</sup> and independently Niessen,<sup>20</sup> with the Sommerfeld quantization conditions of the old quantum theory?

For the same reason that Sommerfeld had excluded the angular quantum number  $l = 0$  for the  $H$  atom—avoidance of electron collision with the nucleus—both Pauli and Niessen excluded electron motion in the nuclear plane of the  $H_2^+$  molecule ion. They then found the lowest admissible quantum state to be  $(n_\xi, n_\eta, n_\varphi) = (0, 1, 1)$ , denoted  $2p\Pi_u$  in molecular spectroscopy, with  $E_0(P, N) = -0.52 R_y$  at  $R_0(P, N) = 5.53 \pm 0.01 r_B$ , depicted by the triangle in the top part of Fig. 7. The QM energy<sup>21</sup> of that quantum state is  $E_0(2p\Pi_u) = -0.27 R_y$  at  $R_0(2p\Pi_u) \approx 8 r_B$ , marked by the solid dot at the minimum of the dotted curve. Since both these energy values are higher than the ground state of a free hydrogen atom, they give rise to *positive* molecular binding energies and thus to spontaneous dissociation,  $H_2^+(2p\Pi_u) \rightarrow H + H^+$ . Qualitatively, Pauli’s and Niessen’s finding of energetic *instability* is borne out by quantum mechanics for this excited state of  $H_2^+$  (Pauli’s argument<sup>4</sup> about “dynamical stability” notwithstanding). The deviation of their historical value ( $\triangle$ ) from the (dotted) QM curve is remarkably small—comparable to those of the CO and SR results for the ground state. Pauli’s and Niessen’s misfortune, though, was that they *misinterpreted* their result as the molecule ion’s ground state—an assessment with fateful consequences in the development of quantum theory.



## C. Discussion

Why do the semiclassical results of the Coulomb oscillator and of SR's quantization deviate from the QM solution of the  $H_2^+$  molecule ion? Strand and Reinhardt explain the deviation of their primitive quantization from QM with effective potential barriers arising from constrictions due to conservation of both the energy  $E$  and the bifocal Runge-Lenz component  $\Omega_c$  (the angular momentum vanishes for the ground state,  $\mathbf{M} = 0$ ). The most drastic consequence of those barriers is the discontinuity of  $E_{el}$  at  $R^*$  (see Fig. 7) and the large deviations at closer proton separation,  $R < R^*$ . While the simulation of quantum mechanical tunneling beyond the semiclassical turning points of librations is adequately achieved by EKB quantization under the isotropic symmetry of a free  $H$  atom,<sup>19</sup> Eq. (19) is less successful under the lower symmetry of  $H_2^+$ . When SR remedy the situation with “unified” semiclassical quantization conditions, then  $E_{el}$  agrees, for all practical purposes, with QM. Those unified quantization condition, going well beyond Eq. (19), are sophisticated in their dependence on  $E_{el}$ ,  $\Omega_c$ , and the hyperbolic turning points  $\eta_{\pm}$ . They will not be discussed here.

The reason for the deviation of the CO results from the QM values is the *neglect* of the electron's *wave* nature in the underlying quantization condition, Eq. (16). In proposing his wave hypothesis de Broglie<sup>22</sup> already showed that the quantization condition of the Bohr model,  $A_n = nh$ , is equivalent to  $n$  standing waves along the  $n$ th Bohr orbit. If  $s$  denotes the position along the Bohr orbit, then the de Broglie wave can be expressed as  $w(s) = \sin[2\pi a_n(s)/h]$ , with the variable  $a_n(s) = (A_n/S_n) \int_0^s ds'$  along the orbit's circumference  $S_n = 2\pi r_n$ . A generalization gives the de Broglie wave of the Coulomb oscillator of a free  $H$  atom in the ground state ( $n = 1$ ),

$$w(z) = \cos[2\pi a(z)/h] \quad (20a)$$

with

$$a(z) = \frac{m}{\phi} \int_0^z v(z') dz' \quad (20b)$$

where  $v(z')$  is the speed from Eq. (2) and  $\phi$  the fold-out factor from Eqs. (4), (9) and (14).

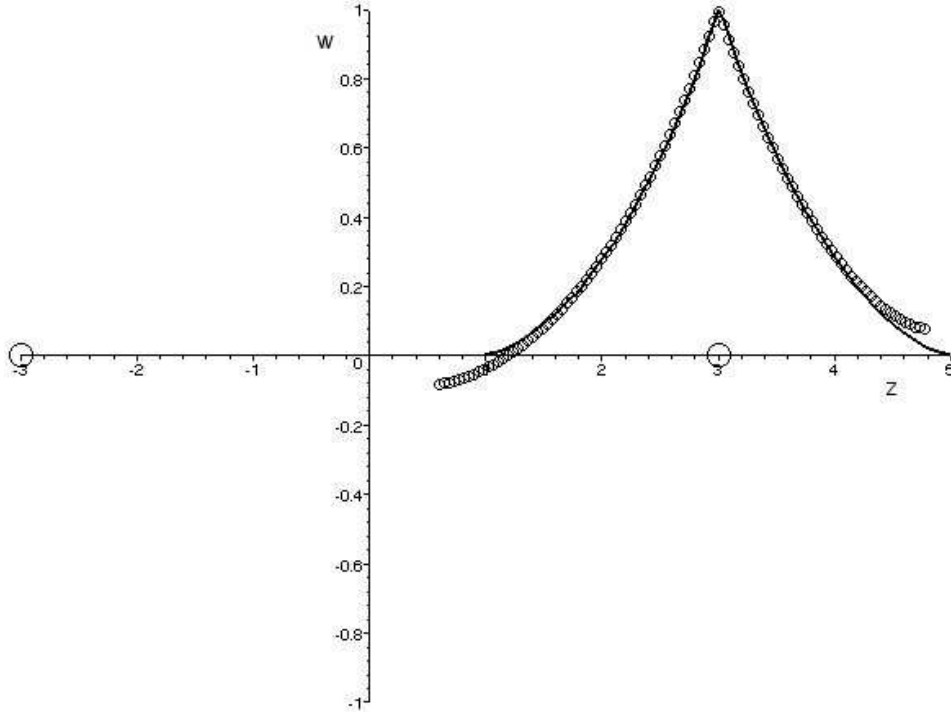


Fig. 8. de Broglie wave of the free  $H$  atom Coulomb oscillator (curve) and of the  $H_2^+$  Coulomb oscillator (small circles) for the same proton separation as in Fig. 5,  $R = 6 r_B$ . Large circles indicate the axial positions of the nuclei.

This de Broglie wave, shown by the line curve in Fig. 8 for a free  $H$  atom positioned at  $+c$ , has peak at the nucleus—like the QM radial wave function—and a node at each turning point. By the above characterization, those turning points are “soft,” and it is their softness that ensures the exact energy of the free atom. However, when Eq. (20ab) is applied to  $H_2^+$  for proton separations beyond the bifurcation value,  $R > \check{R}$ , with axial speed from Eq. (8ab) and integration away from the occupied nucleus,  $\int_c^z \dots$ , then the de Broglie wave is found to be “truncated” (no nodes) at both the outer and inner turning point (see Fig. 8, small circles). Those turning points are “hard” and give rise to incorrect energies. Qualitatively, an augmentation of the truncated de Broglie wave with (exponential) “tunneling tails,” determined by the negative kinetic energy in the classically “forbidden” region,

would “soften” the turning points. This would give rise to an *effective* far turning point farther out,  $C_{eff} > C$ , and accordingly raise the CO energy, Eq. (7), toward the QM result.

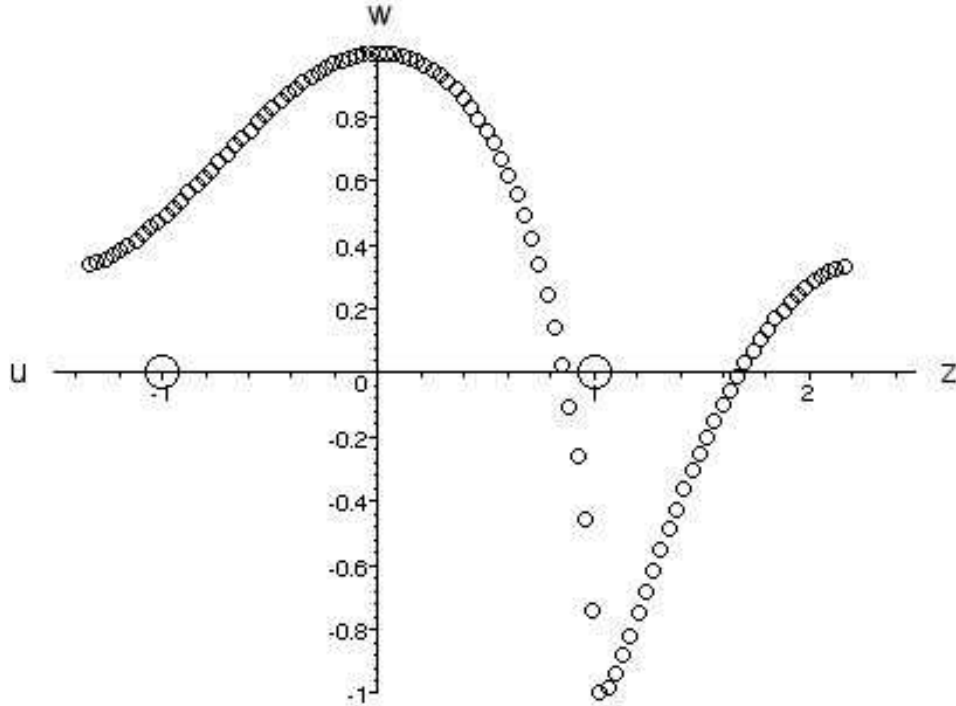


Fig. 9. de Broglie wave of the  $H_2^+$  Coulomb oscillator along axial distance  $OC$  from Fig. 4 (right side of graph) and lateral distance  $OB$  (left side). Large circles indicate the axial positions of the nuclei, here with the same separation as in Fig. 6,  $R = 2 r_B$ .

When the proton separation is below bifurcation,  $R < \tilde{R}$ , then Eq. (20b) should be integrated from the midpoint 0 in both the axial and lateral direction rather than favoring one nucleus with the crest of the de Broglie wave. Again, the de Broglie wave is found to be truncated at the axial and lateral turning points,  $C$  and  $B$ , respectively (see Fig. 9). An exception exists for the proton separation  $R^*$ . The de Broglie wave, shown in Fig. 10, then has a minimum at both turning points,  $w(C) = w(B) = -1$ , according to action values of  $A_z = \frac{3}{4}h$  and  $A_y = \frac{1}{4}h$ . Such turning points seem to be “benign”—reminiscent of the soft turning points in the free-atom case—and cause the

CO energy  $E_{el}(R^*)$  in Fig. 7 to be *exact*. At still smaller proton separation,  $R < R^*$ , the de Broglie wave is truncated again (not shown). The limit  $R = 0$  corresponds to a Coulomb oscillator in the free  $He^+$  ion which, like in the free  $H$  atom for  $R = \infty$ , has de Broglie nodes at the turning points and an exact energy value.

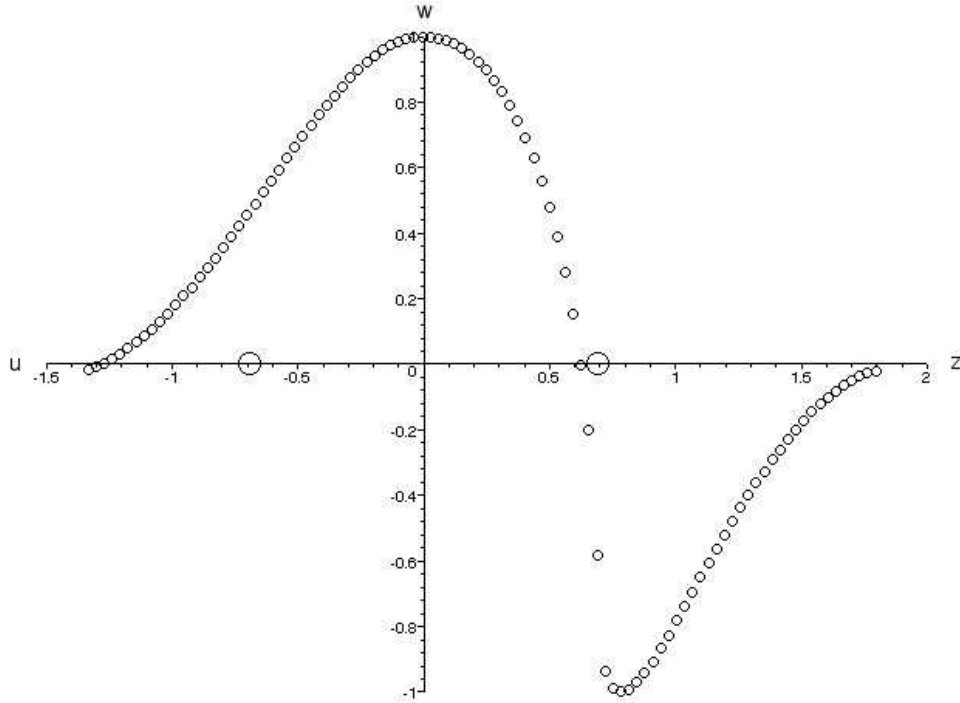


Fig. 10. Same as Fig. 9 but for the proton separation  $R^* = 1.38 r_B$  where the semiclassical energy is exact.

If the explanation that the CO energy  $E_{el}(R)$  deviates from the QM curve because of the *neglect* of *wave* effects is valid, then this sheds new light on the SR results. The opposite sign of the CO and SR deviations then suggests that SR's primitive EBK quantization, while appropriate for a free atom, simulates *too much wave effects* under the lower symmetry of the  $H_2^+$  molecule ion. However, the *average* of both those semiclassical quantizations seems to be an excellent compromise, as evidenced by the close agreement of the corresponding total energy ( $\diamond$ ) with the (dashed) QM curve in Fig. 7.

In conclusion, semiclassical quantization can rise to Gutzwiller’s challenge and “explain” the chemical bond in the paradigm molecule,<sup>23</sup>  $H_2^+$ , by a combination of classical mechanics, quantization, and moderate wave effects.

#### IV. ACKNOWLEDGMENTS

I thank Duane Siemens and Ernst Mohler for valuable discussions. Many thanks to Preston Jones for help with computer integration and graphics. I also thank Professor Gutzwiller for advice and his kind encouragement.

#### V. APPENDIX A: QUANTIZATION

By Eq. (4) the action integral of the atomic Coulomb oscillator is

$$A = \frac{1}{\phi} \oint p_z dz = -\frac{4e}{\phi} \sqrt{2Zm} \int_{\Gamma}^0 \sqrt{\frac{1}{z} - \frac{1}{\Gamma}} dz. \quad (4')$$

For a comparison with integral tables we change notation to  $x = z$  and use the abbreviation  $a = -1/\Gamma$ . Then

$$\int \sqrt{\frac{1}{z} - \frac{1}{\Gamma}} dz = \int \sqrt{\frac{1}{x} + a} dx = \int \frac{\sqrt{X}}{x} dx \quad (21)$$

with  $X = ax^2 + x$ . Integration tables give

$$\int \frac{\sqrt{X}}{x} dx = \sqrt{X} + \frac{1}{2} \int \frac{dx}{\sqrt{X}}. \quad (22)$$

The first term on the rhs, evaluated at the limits of the  $\int_{\Gamma}^0$  integration, vanishes. The last integral in Eq. (22), tabulated as

$$\int \frac{dx}{\sqrt{X}} = (-\sqrt{\Gamma}) \arcsin(1 - 2x/\Gamma), \quad (23)$$

and evaluated at the limits,  $x = 0$  and  $x = \Gamma$ , contributes

$$- [\arcsin(1) - \arcsin(-1)] \sqrt{\Gamma} = -\pi \sqrt{\Gamma}. \quad (24)$$

Combining Eqs. (4'), (22) and (24), together with a fold-out factor  $\phi = 2$ , gives the action integral, to be equated with the Sommerfeld quantization condition,

$$A_n = -\frac{4e}{\phi} \sqrt{2Zm} \frac{1}{2} (-\pi \sqrt{\Gamma}) = nh. \quad (25)$$

We square Eq. (25) and solve for the amplitude of the quantized Coulomb oscillator,

$$\Gamma_n = 2 \frac{r_B}{Z} n^2, \quad (26)$$

in terms of the Bohr radius  $r_B$ .

## VI. APPENDIX B: DATA

TABLE I. Electronic ground-state energy  $E_{el}$  for various nuclear separations  $R$  of the  $H_2^+$  molecule from quantum-mechanical calculations (QM, Ref 21), the “primitive” semiclassical quantization of Strand and Reinhardt (SR, Ref. 15), and the present Coulomb-oscillator approach (CO).

R ( <i>a.u.</i> )	QM ( $R_y$ )	SR ( $R_y$ )	CO ( $R_y$ )
0.00	-4.00	-4.00	-4.00
0.25	-3.80	-4.75	-3.35
0.50	-3.47	-4.27	-3.12
0.75	-3.11	-3.76	-2.93
1.00	-2.90	-3.34	-2.81
1.25	-2.68	-3.07	-2.67
1.50	-2.50	-2.19	-2.55
1.75	-2.34	-2.09	-2.45
2.00	-2.21	-1.99	-2.36
2.50	-1.99	-1.79	-2.18
3.00	-1.82	-1.66	-2.02
3.50	-1.69	-1.56	-1.87
4.00	-1.59	-1.49	-1.75
5.00	-1.45	-1.40	-1.54
6.00	-1.36	-1.33	-1.38
8.00	-1.26	-1.25	-1.27
10.00	-1.20	-1.20	-1.20
12.00	-1.17	-1.17	-1.17

## References

- <sup>1</sup>Other failures were its inability to give the brightness of spectral lines and the unsuccessful extension to the *He* atom.
- <sup>2</sup>M. Jammer, *The Conceptual Development of Quantum Mechanics* (McGraw-Hill, New York, 1966), p. 129.
- <sup>3</sup>Instead of the traditional notation  $k$  for the angular quantum number in the old quantum theory, we will use the letter  $l$  ( $= k$ ) to facilitate the connection with quantum mechanics.
- <sup>4</sup>W. Pauli, “Über das Modell des Wasserstoffmolekülions,” *Annalen der Physik* **68**, 177-240 (1922). A history of Pauli’s thesis is given by C. P. Enz, “No Time to be Brief: A Scientific Biography of Wolfgang Pauli” (Oxford UP, 2002), pp. 63-74.
- <sup>5</sup>M. C. Gutzwiller, *Chaos in Classical and Quantum Mechanics* (Springer, New York, 1990), p. 36.
- <sup>6</sup>A. Sommerfeld, “Zur Quantentheorie der Spektrallinien,” *Annalen der Physik*, **51**, 1-94 (1916).
- <sup>7</sup>This length of semiminor axis has been modified from Sommerfeld’s original expression,  $b_{nl} = (r_B/Z)nk$ , to achieve agreement with expressions from quantum mechanics.
- <sup>8</sup>If the nuclear charge is uniformly distributed, then  $Z'(r) = (r/r_N)^3Z$ , and the electron’s motion inside the nucleus is harmonic.
- <sup>9</sup>M. Bucher, D. Elm and D. P. Siemens, “Average position in Kepler motion,” *Am. J. Phys.* **66**, 929-930 (1998).
- <sup>10</sup>L. Pauling and E. B. Wilson, *Introduction to Quantum Mechanics* (Dover, New York, 1935) p. 144.
- <sup>11</sup>Although almost all quantum texts use the weaker statement “at the nucleus.”
- <sup>12</sup>M. Bucher, “The electron inside the nucleus: An almost classical derivation of isotropic hyperfine interaction,” *Eur. J. Phys.* **21**, 19-22 (2000).



- <sup>13</sup>A. Einstein, “*Zum Quantenansatz von Sommerfeld und Epstein,*” Verh. Dtsch. Phys. Ges. **19**, 82-92 (1917). A summary with modern comments is given by A. D. Stone, “*Einstein’s unknown insight and the problem of quantizing chaos,*” Phys. Today, Aug. 2005, pp. 37-43.
- <sup>14</sup>Eq. (3), introduced as Sommerfeld quantization for familiarity’s sake, is also an Einstein quantization condition.
- <sup>15</sup>M. P. Strand and W. P. Reinhardt, “*Semiclassical quantization of the low lying electronic states of  $H_2^+$ ,*” J. Chem. Phys. **70**, 3812-27 (1979).
- <sup>16</sup>The (one-center) Runge-Lenz vector,  $\mathbf{\Omega} = \mathbf{v} \times \mathbf{L} - Ze^2\mathbf{r}/r$ , of a Sommerfeld orbit of angular momentum  $\mathbf{L}$  has a magnitude proportional to the ellipse’s eccentricity  $\varepsilon$  and points from the nucleus toward the perihelion; see J. Morehead, “*Visualizing the extra symmetry of the Kepler problem,*” Am. J. Phys. **73**, 234-239 (2005). For a Coulomb oscillator ( $L = 0$ ,  $\varepsilon = 1$ ),  $\mathbf{\Omega}$  oscillates and thus is *not conserved*. Neither is  $\Omega_c$  of the two-center *Coulomb oscillator* conserved; see H. A. Erikson and E. L. Hill, “*A Note on the one-electron state of diatomic molecules,*” Phys. Rev. **75**, 29-31 (1949); and also C. A. Coulson and A. Joseph, “*A constant of the motion for the two-center Kepler problem,*” Int. J. Quantum Chem. **1**, 337-347 (1967).
- <sup>17</sup>The trajectory will eventually revisit an arbitrarily close neighborhood of any previous point.
- <sup>18</sup>Ref. 5, pp. 207-215.
- <sup>19</sup>L. J. Curtis and D. G. Ellis, “*Use of the Einstein-Brillouin-Keller action quantization,*” Am. J. Phys. **72**, 1521-1523 (2004).
- <sup>20</sup>K. F. Niessen, “*Zur Quantentheorie des Wasserstoffmolekülions,*” Annalen der Physik **70**, 129-134 (1923).
- <sup>21</sup>M. M. Madsen and J. M. Peek, At. Data **2**, 171 (1971); E. Teller and H. L. Sehlin, in *Physical Chemistry, An Advanced Treatise* (Academic, New York, 1970), Vol. **5**, p. 35.
- <sup>22</sup>L. de Broglie, “*Ondes et quanta,*” Comptes Rendus **177**, 507-510 (1923).

<sup>23</sup>K. Ruedenberg, "*The physical nature of the chemical bond,*" Rev. Mod. Phys. **34**, 326-276 (1962).

2-24-2006

# Coulomb oscillation in the hydrogen atom and molecule ion

Manfred Bucher

Physics Department, California State University, Fresno  
Fresno, California 93740-8031

## Abstract

Semiclassical oscillation of the electron through the nucleus of the  $H$  atom yields both the exact energy and the correct orbital angular momentum for  $l = 0$  quantum states. Similarly, electron oscillation through the nuclei of  $H_2^+$  accounts for a stable molecule ion with energy close to the quantum mechanical solution. The small discrepancy arises from the neglect of the electron's wave nature.

PACS numbers: 03.65.Sq, 31.10.+z, 31.20.Pv

## I. INTRODUCTION

Two of the reasons why the old quantum theory of Bohr and Sommerfeld was abandoned in the mid 1920s were the theory's failure to give the correct multiplet structure of the hydrogen atom and the stability of the hydrogen molecule ion,  $H_2^+$ .<sup>1</sup> The old vector model of angular momentum<sup>2</sup> gave, for a given principal quantum number  $n$ , sublevels with angular quantum numbers  $l = 1, 2, \dots, n$ .<sup>3</sup> Spectroscopic evidence, however, showed multiplicities of spectral line splitting in a magnetic field according to  $l = 0, 1, \dots, n - 1$ . Max Jammer, in his review,<sup>2</sup> notes that “the old quantum theory could never resolve this inconsistency.”

A treatment of the hydrogen molecule ion with Sommerfeld's quantization conditions had been Wolfgang Pauli's doctoral thesis of 1922.<sup>4</sup> Pauli found its molecular binding energy to be positive (non-binding)—contrary to (later) experimental findings. Martin Gutzwiller<sup>5</sup> thinks that “the solution of this problem can be rated, with only slight exaggeration, as the most important in quantum mechanics, because if an energy level with a [more] negative value [than of a free hydrogen atom] can be found, then the chemical bond between two protons by a single electron has been explained.”

Both dilemmas of the old quantum theory can be resolved, though, with a single extension: an oscillation of the electron through the nucleus (nuclei) of the atom (molecule). In essence this solution is already formally included in Sommerfeld's theory of the hydrogen atom<sup>6</sup> but was explicitly omitted by Sommerfeld and his school as being *unphysical*. The case in point, obtained with Sommerfeld's quantization conditions for radial and angular motion, is a quantum state with zero angular action, characterized by an angular quantum number  $l = 0$ . What is its orbit?

The geometry of an  $nl$  Sommerfeld ellipse is given by its semimajor axis,  $a_{nl} = (r_B/Z)n^2$ , and semiminor axis,  $b_{nl} = (r_B/Z)n\sqrt{l(l+1)}$ .<sup>7</sup> Here  $r_B = h^2/4\pi^2me^2$  is the Bohr radius in terms of fundamental constants, serving as an atomic distance unit, and  $Ze$  is the nuclear charge. An  $(n, 0)$  orbit is thus a line ellipse with its nuclear focus at one end and its empty focus at the other. This case was regarded as unphysical because of the electron's collision with the nucleus—an uncritical adaptation from celestial mechanics. A closer inspection confirms that a line ellipse with *terminal* nuclear focus is indeed unphysical—but for quite a different reason!

Figure 1 Here

Fig. 1. Partial trajectory of an extranuclear orbit  $XX'$  and of a penetrating orbit  $PP'$  through nucleus  $N$ . The dotted line  $S$  shows the major symmetry axis of  $XX'$ .

Leaving quantization conditions momentarily aside, what would happen if we *continuously* decrease an angular quantum number  $\lambda$  while keeping the principal quantum number  $n$  constant? We then would get more and more slender ellipses with the same length of major axis,  $2a_n$ . By basic electric theory, the nuclear Coulomb potential outside a *finite-size* nucleus  $N$  is given by the point potential as if all nuclear charge,  $+Ze$ , was concentrated at the center of the nucleus. This holds as long as the electron orbit stays outside the nucleus. Two borderline cases are illustrated in Fig. 1. For a very small  $\lambda$  value, say  $0 < \lambda_X \ll 1$ , we obtain a very slender elliptical orbit with partial trajectory  $XX'$  about the nucleus. Further decrease of  $\lambda$  to  $\lambda_P < \lambda_X$  causes an intrusion of the electron into the finite nucleus of radius  $r_N$  (see trajectory  $PN$  in Fig. 1). Once inside, at a distance  $r < r_N$  from the center, then, by Gauss's law, only a fraction of the nuclear charge,  $Z'(r)e < Ze$ , acts on the electron via centripetal force.<sup>8</sup> Accordingly, the electron's exit trajectory  $NP'$  is no longer symmetric to its approach trajectory  $PN$  with respect to the major axis  $S$  of the (partial) ellipse  $XX'$ . In the extreme case of a head-on penetration of the nucleus,  $\lambda = 0$ , there is no centripetal force at all! The electron will then, with almost constant speed, traverse the nucleus, continue, with decreasing speed, to the opposite turning point of its line orbit and revert its motion periodically. We want to call the electron's straight-line oscillation in the Coulomb potential of a finite-size nucleus a "*Coulomb oscillator*."

## II. HYDROGEN ATOM

For the formal treatment of the non-relativistic Coulomb oscillator we designate the  $z$  axis along the line orbit, with turning points at  $z = \pm\Gamma$  and nuclear position at  $z = 0$  (see Fig. 2). The electron's total energy  $E$  at position  $z$  must equal the potential energy at a turning point,

$$E = \frac{1}{2}mv^2 - \frac{Ze^2}{|z|} = -\frac{Ze^2}{\Gamma}. \quad (1)$$

This gives the electron's speed along the  $z$  axis,

$$v = \pm e \sqrt{\frac{2Z}{m}} \sqrt{\frac{1}{|z|} - \frac{1}{\Gamma}}. \quad (2)$$

Figure 3 displays its dependence on the axial position as a two-wing curve cusped at the nucleus. Atomic units (*a.u.*) are used, that is, the Bohr radius  $r_B$  and the “Bohr speed”  $v_B = 2\pi e^2/h = \alpha c$ —the electron speed in the ground-state Bohr orbit of the  $H$  atom—with fine-structure constant  $\alpha \approx 1/137$  and speed of light  $c$ . The curve’s wing along the positive  $z$  axis,  $|z| = r$ , gives the *radial* speed,  $v_r(r) = |v(z)|$ , necessary for Sommerfeld’s *radial* quantization condition,

$$\oint p_r dr = m \oint v_r(r) dr = n_r h. \quad (3)$$

Here  $p_r$  is the radial momentum,  $n_r = 1, 2, \dots$  is the radial quantum number, and  $h$  is Planck’s quantum of action. Integration is over one period of the radial motion,  $z = +\Gamma \rightarrow 0 \rightarrow +\Gamma$ . Graphically, the radial quantization is illustrated in Fig. 3 by the area under *one* wing of the speed curve. For a line orbit,  $l = 0$ , the radial quantum number equals the principal quantum number,  $n \equiv n_r + l = n_r$ .

In order to express the radial quantization in terms of *axial* motion we employ a “fold-out factor,”  $\phi = 2$ , to compensate for the doubling of integration range in the extension from the radial one-wing speed curve to the axial two-wing curve. The quantization is thus restated,

$$\frac{1}{\phi} \oint p_z dz = \frac{m}{\phi} \oint v(z) dz = n_z h, \quad (3')$$

with axial quantum number  $n_z = n_r = n$  and integration over the axial double-wing range,  $z = +\Gamma \rightarrow -\Gamma \rightarrow +\Gamma$ . By symmetry we can restrict the axial action integral to one quarter of the oscillation, say  $z = +\Gamma \rightarrow 0$ ,

$$\frac{1}{\phi} \oint p_z dz = -\frac{4m}{\phi} \int_{\Gamma}^0 v(z) dz = -\frac{4e}{\phi} \sqrt{2Zm} \int_{\Gamma}^0 \sqrt{\frac{1}{z} - \frac{1}{\Gamma}} dz = nh. \quad (4)$$

Here the electron’s motion in the negative  $z$  direction is accounted for by the negative sign. Although the electron’s speed through a point nucleus diverges,  $v(0) = \infty$ , the action integral, Eq. (4), stays finite and determines

the quantized amplitude  $\Gamma_n$  of the Coulomb oscillator. Graphically the amplitude  $\Gamma_n$  must be such that it stretches the speed curve horizontally to the extent that the area under one wing,  $A_n = nh$ , represents the quantized action. The analytic solution, derived in Appendix A, is

$$\Gamma_n = 2\frac{r_B}{Z}n^2. \quad (5)$$

Inserting Eq. (5) into Eq. (1) yields the quantized energy,

$$E_n = -\frac{Z^2e^2}{\Gamma_n} = -\frac{Z^2}{n^2}R_y, \quad (6)$$

in terms of the Rydberg energy unit,  $R_y = 2\pi^2me^4/h^2 = 13.6 \text{ eV}$ , and in agreement with the energy of the  $n$ th Bohr orbit.

Note that Eq. (5) gives the amplitude of the  $n$ th Coulomb oscillator as *twice* the radius of the  $n$ th Bohr orbit or of the semimajor axis of an  $nl$  Sommerfeld ellipse,  $r_n = a_{nl} = (r_B/Z)n^2$ . For comparison, the time-average radial distance of a Kepler orbit<sup>9</sup> of major and minor semiaxes  $a$  and  $b$ , respectively, is  $\langle r \rangle_t = (3a^2 - b^2)/(2a)$ . A line ellipse ( $b = 0$ ) has then  $\langle r \rangle_t = \frac{3}{2}a$ . Applied to an  $nl$  Sommerfeld orbit,<sup>9</sup> its average size,  $\langle r_{nl} \rangle_t = (r_B/Z)[3n^2 - l(l+1)]/2$ , is in agreement with the corresponding quantity from quantum mechanics,<sup>10</sup>  $\langle r_{nl} \rangle = \int \psi^* r \psi d^3r$ . Thus the time-average radial distance of a Coulomb oscillator is  $\langle r_{n0} \rangle_t = \frac{3}{2}(r_B/Z)n^2$ . For the ground state of the hydrogen atom,  $n = 1$ , this gives  $\langle r_{10} \rangle_t = \frac{3}{2}r_B$ , as is well-known from quantum mechanics.<sup>10</sup>

The concept of the electron's semiclassical Coulomb oscillation is consistent with the Fermi-contact term of hyperfine interaction for  $l = 0$  states, which arises from the presence of the electron *inside* the nucleus. This is familiar from quantum mechanics<sup>11</sup> and can be interpreted semiclassically as a local-field effect.<sup>12</sup>

To be sure, the extension of Sommerfeld's theory by the Coulomb oscillator resolves the discrepancy of the old quantum theory with spectroscopy, mentioned above, only at the *low* end of angular quantum numbers,  $l = 0$ . The resolution at the high end—repeal of the circular Bohr orbit,  $l \neq n$ —involves an analysis in terms of space quantization which is beyond the scope of the present study.

### III. HYDROGEN MOLECULE ION

#### A. Formalism

A hydrogen molecule ion,  $H_2^+$ , consists of two proton nuclei and one electron. We assume, in adiabatic approximation, the protons located at fixed positions  $z = \pm c$  on the molecular axis (see Fig. 4). The term ‘‘Coulomb oscillator’’ denominates again the motion of a point electron, now along either the line through the protons ( $z$  axis) and with turning points  $\pm C$ , or along the perpendicular line through the midpoint ( $y$  axis) with turning points  $\pm B$ . The molecule ion’s total energy  $E$  at any position on the axis,  $-C \leq z \leq +C$ , must equal the potential energy at the turning point  $C$ ,

$$E = \frac{1}{2}mv^2 - \frac{e^2}{|z+c|} - \frac{e^2}{|z-c|} + \frac{e^2}{2c} = -\frac{e^2}{C+c} - \frac{e^2}{C-c} + \frac{e^2}{2c}. \quad (7)$$

For electron positions beyond the protons,  $z > c$ , this gives an electron speed

$$v_{out} = \pm \frac{2e}{\sqrt{m}} \sqrt{\frac{z}{z^2 - c^2} - \frac{C}{C^2 - c^2}}. \quad (8a)$$

For positions between the protons,  $0 < z < c$ , the corresponding speed is

$$v_{in} = \pm \frac{2e}{\sqrt{m}} \sqrt{\frac{c}{c^2 - z^2} - \frac{C}{C^2 - c^2}}. \quad (8b)$$

The speed expressions will be used in the action integral,

$$\frac{1}{\phi} \oint p_z dz = \frac{2m}{\phi} \int_C^{-C} v(z) dz = A_z = A_{out} + A_{in}, \quad (9)$$

with outer contribution

$$A_{out} = \frac{2m}{\phi} \left[ \int_C^c v_{out}(z) dz + \int_{-c}^{-C} v_{out}(z) dz \right] \quad (10a)$$

and inner contribution

$$A_{in} = \frac{2m}{\phi} \int_c^{-c} v_{in}(z) dz. \quad (10b)$$



Here  $\phi$  is a fold-out factor to be specified below.

If the conditions are such that the electron swings along the  $z$  axis through the midpoint 0, that is,  $v_{in}(0) > 0$ , then there exists also an oscillation along the  $y$  axis with lateral speed  $u$ , having the same total energy,

$$E = \frac{1}{2}mu^2 - \frac{2e^2}{\sqrt{y^2 + c^2}} + \frac{e^2}{2c} = -\frac{2e^2}{\sqrt{B^2 + c^2}} + \frac{e^2}{2c}. \quad (11)$$

Equal energy at the axial and lateral turning points,  $E(C) = E(B)$ , Eqs. (7) and (11), determines the latters' geometric dependence,

$$B = \sqrt{C^2 + \frac{c^4}{C^2} - 3c^2}. \quad (12)$$

Solving Eq. (11) for the lateral speed,

$$u = \pm \frac{2e}{\sqrt{m}} \sqrt{\frac{1}{\sqrt{y^2 + c^2}} - \frac{1}{\sqrt{B^2 + c^2}}}, \quad (13)$$

provides the integrand of the action integral over a lateral oscillation,

$$A_y = \frac{1}{\phi} \oint p_y dy = \frac{2m}{\phi} \int_B^{-B} u(y) dy. \quad (14)$$

Subtraction of the protons' mutual repulsion from the total energy  $E$  of axial or lateral motion, Eqs. (7) and (11), gives the *electronic* energy,

$$E_{el} = E - \frac{e^2}{R}, \quad (15)$$

in its dependence on the proton separation,  $R = 2c$ . This brackets the molecular problem with known atomic results, Eq. (6), in the limits of  $R = \infty$  (free  $H$  atom,  $Z = 1$ ) and  $R = 0$  (free  $He^+$  ion,  $Z = 2$ ). For those cases, as well as any proton-proton distance  $R$  between, we keep the action constant,

$$A = A_z + A_y = nh. \quad (16)$$

Equation (16) is the *Einstein* quantization condition<sup>13</sup>—a generalization of Sommerfeld's quantization over separable variables—where the *quantum sum* equals the sum of action integrals over topologically independent paths in phase space.<sup>14</sup>

Here we treat the molecule ion only in its *ground state*,  $n = 1$ . Analytic solutions of the action integrals, Eqs. (10ab) and (14), are complicated due to elliptic functions. We therefore integrate numerically and visualize the integrals by the area under the corresponding speed curves. The bold curve in Fig. 5 shows the axial electron speed  $v(z)$  for a *far* proton separation,  $R = 6 r_B$ . The electron, in its semiclassical motion, then oscillates only about (and through) the right proton. The area under the speed curve, Eq. (8ab), proportionally represents the ground state's unity of action,  $m \oint v(z) dz = \phi h$ , with a fold-out factor  $\phi = 2$  in analogy to the free-atom case, Eq. (4). The thin curve shows, for comparison, the axial electron speed in a free  $H$  atom—familiar from Fig. 3—centered at the same proton position,  $+c$ . The pull from the left proton (at  $-c$ ) on the oscillating electron can be seen by the distortion of the speed function  $v(z)$  and the redistribution of the area under the curve.

When, with closer proton separation  $R$ , as in Fig. 6, the electron swings past the midpoint 0, then the single-cusp speed curve  $v(z)$  from Fig. 5—akin in shape to letter  $\Lambda$ —becomes double-cusped (akin to letter M) and symmetric with respect to the bisector ( $y$  axis). Now there is also a lateral oscillation with speed  $u(y)$  having the same total energy  $E$ . The equality of  $E$  in both cases can be seen in Fig. 6 by the equality of axial and lateral speed at the midpoint,  $v(0) = u(0)$ —a position where the electron experiences the same potential in either case. For convenience the lateral speed  $u(y)$ , though perpendicular to the proton axis, is displayed in Fig. 6 together with the axial speed  $v(z)$ . The lateral speed curve  $u(y)$ , drawn dotted, is readily recognized by its dome shape ( $\cap$ ). At the bifurcation value of the proton separation,  $\check{R}$ , where the electron starts swinging though the midpoint 0, the axial speed curve  $v(z)$  changes from its one-centered  $\Lambda$  shape to a two-centered M shape. The *area* under the axial speed curve then abruptly doubles,  $M(\check{R} - \delta) \approx 2\Lambda(\check{R} + \delta)$ , upon a very small change in proton separation,  $\delta \ll \check{R}$ . In order to keep the action integral continuous at  $\check{R}$ , the sudden area doubling is compensated by a corresponding doubling of the fold-out factor from  $\phi = 2$  for  $R > \check{R}$  to  $\phi = 4$  for  $R < \check{R}$ . The same fold-out factor,  $\phi = 4$ , must be used for the lateral action integral  $A_y$ , Eq. (14), as will become clear shortly.

The unity of action,  $A = 1h$ , is visualized again in Fig. 6. To this end we compare the right half of the bold M-shape curve of axial electron speed in the molecule with the thin curve  $\Lambda(H)$  of the axial speed in a free  $H$  atom positioned at the right nucleus,  $+c$ . Due to attraction from the left nucleus,

the right wing of the M curve is smaller than that of  $\Lambda(H)$  by the area of lobe  $L$ . On the other hand, the left flank of the  $\Lambda(H)$  curve that extends over the negative  $z$  axis is smaller than the left wing of the lateral speed curve  $\cap$  by the area of slice  $S$ . The area under the free-atom curve is then

$$\Lambda(H) \approx \frac{1}{2}M + L + \frac{1}{2}\cap - S. \quad (17a)$$

The areas of lobe and slice are comparable,

$$L \approx S. \quad (17b)$$

When the tiny notch to the right of the saddle point of M is taken into account, then the approximations (17ab) become equations and combine to

$$M + \cap = 2\Lambda(H). \quad (18)$$

The area under both the axial and lateral speed curves is thus four times the area under *one* wing of the free-atom curve,  $M + \cap = 4 \times \frac{1}{2}\Lambda(H)$ . Since the latter represents one quantum of action,  $h$ , the combined area  $M + \cap$  visualizes its *double* fold-out,  $\phi = 4$ .

With very close proximity of the nuclei,  $R \rightarrow 0$ , the crests of the M curve start merging while its saddle point,  $v(0)$ , keeps rising. In the  $R = 0$  limit of fusing nuclei the axial electron speed becomes that of a free  $He^+$  ion,  $M \rightarrow \Lambda(He^+)$ , familiar from Fig. 3. Concurrently, the lateral speed curve  $\cap$  rises at its peak,  $u(0) = v(0)$ , and narrows at its base until it, too, turns into the speed curve of the free  $He^+$  ion,  $\cap \rightarrow \Lambda(He^+)$ . In the  $R = 0$  limit the three curves merge,  $M(0) = \cap(0) = \Lambda(He^+)$ .

The results of the Coulomb-oscillator approach will be compared with another semiclassical calculation of  $H_2^+$ , by Strand and Reinhardt.<sup>15</sup> These authors, like Pauli,<sup>4</sup> separate the equation of motion in spheroidal coordinates,  $\xi = (r_+ + r_-)/2c$ ,  $\eta = (r_+ - r_-)/2c$  and  $\varphi$  by virtue of the constants of the motion: total energy  $E$ , angular momentum  $\mathbf{M}$  about the  $z$  axis, and a component of the bifocal Runge-Lenz vector,  $\Omega_c$ .<sup>16</sup> Here  $r_+$  ( $r_-$ ) is the distance of the electron from the nucleus at  $+c$  ( $-c$ ). Strand and Reinhardt (SR) solve the ensuing one-dimensional differential equations with classical Poisson-bracket techniques. They find the electron's trajectories conditionally periodic<sup>17</sup> and regionally confined due to restrictions from  $E$ ,  $\mathbf{M}$  and  $\Omega_c$ . However, unlike Pauli, who used Sommerfeld quantization, SR employ the Einstein-Brillouin-Keller (EBK) quantization conditions,

$$A_j = \oint p_j dj = (n_j + \frac{1}{2})h, \quad j = \xi, \eta \quad (19ab)$$

and

$$A_\varphi = \oint p_\varphi d\varphi = n_\varphi h. \quad (19c)$$

The background of EBK quantization touches on the foundations of classical and quantum mechanics.<sup>18</sup> For the present purpose its essential rationale may be summarized as follows: A semiclassical treatment involves turning points of radial, or other librating motion. Any tunneling through “forbidden” regions of negative kinetic energy is ruled out. Viewed in terms of the quantum mechanical WKB (Wentzel-Kramers-Brillouin) approximation, the hard reflection of a wavefunction at a turning point corresponds to a so-called “loss” of phase (phase shift by  $\pi$ ) compared to the soft reflection caused by tunneling (phase shift by  $\pi/2$ ). This shortcoming can be remedied with EBK quantization conditions by addition of a value of  $1/4$ , for each librational turning point, to the corresponding quantum number. Such is the case for the electron’s elliptical and hyperbolic librations in the above quantization, Eq. (19ab), but not for a rotation about the  $z$  axis, Eq. (19c). Strand and Reinhardt call these quantization conditions “primitive” to distinguish them from more sophisticated ones, specified below.

A semiclassical treatment of a free  $H$  atom with EBK quantization has recently been presented in these pages.<sup>19</sup> In this case the isotropic symmetry permits a separation of variables in spherical coordinates,  $r$ ,  $\theta$  and  $\varphi$ , and the EBK quantization conditions are like Eqs. (19abc) except for  $j = r, \theta$ . The atomic ground state is characterized by the quantum numbers  $(n_r, n_\theta, n_\varphi) = (0, 0, 0)$ . Accordingly, the action in the atom’s ground state,  $A_1 = 1h$ , is attributed only to tunneling at the radial and latitudinal turning points (the former being the nucleus). Applying EBK quantization to the ground state of  $H_2^+$ , denoted  $1s\Sigma_g$  in molecular spectroscopy, SR likewise assign the quantum numbers  $(n_\xi, n_\eta, n_\varphi) = (0, 0, 0)$ .

## B. Results

Energies of the Coulomb oscillator (CO), in adiabatic dependence on the proton separation, are listed in Appendix B and shown in Fig. 7 in com-

parison with exact quantum mechanical (QM) results and the semiclassical calculation by SR.<sup>15</sup> The lower part of Fig. 7 shows the electronic energy  $E_{el}(R)$  of the ground state,  $1s\Sigma_g$ . At *large* proton separations,  $R > 6 r_B$ , both the SR calculation (circles) and the CO approach (crosses) agree excellently with the exact QM values (curve). This is the situation where the electron stays near one nucleus (see Fig. 5). As Fig. 7 further shows, such agreement ceases once the classical electron motion leads beyond the molecular bisector, which happens for proton separations below the bifurcation value,  $R < \tilde{R} \approx 5.57 r_B$  (see Fig. 6). Interestingly, the deviations of CO and SR from QM are opposite over the entire range. The SR results are *discontinuous* at a certain proton separation,  $R^* \approx 1.38 r_B$ . Remarkably, at (or near) that value,  $R^*$ , the CO energy crosses the curve of the QM solution.

Adding to the electronic energy  $E_{el}$  the proton-proton repulsion gives the *total* energy  $E$ , Eq. (15). The middle part of Fig. 7 shows by the dashed curve the exact total energy  $E(R)$  of the  $1s\Sigma_g$  ground state, obtained from QM and, by symbols, the corresponding CO and SR values. The solid dot at the minimum of the curve shows the QM equilibrium energy, in agreement with experiment,  $E_0 = -1.20 R_y$ , and the equilibrium internuclear distance,  $R_0 = 2.00 r_B$ . The CO energy ( $\times$ ) comes out too low, due to the inaccuracy of its  $E_{el}$ , with an equilibrium value  $E_0(CO) \approx -1.38 R_y$  at  $R_0(CO) \approx 2.5 r_B$ . Conversely, the SR energy ( $\square$ ) comes out too high with  $E_0(SR) \approx -1.05 R_y$  at  $R_0(SR) \approx 5 r_B$ . Since the CO and SR results deviate about equal and oppositely from QM, their *average* ( $\diamond$ ) is close to the exact values with a minimum of  $E_0[\frac{1}{2}(CO + SR)] \approx -1.19 R_y$  at  $R_0[\frac{1}{2}(CO + SR)] \approx 2.5 r_B$ .

The molecular binding energy is the difference of  $E$  in the molecule and in the constituting atoms, here,  $E_0(H_2^+) - E(H)$ . The energy of a free hydrogen atom,  $E(H) = -1 R_y$ , is indicated in Fig. 7 by the fine horizontal line. Both semiclassical treatments, CO and (barely) SR, yield molecular binding energies with *negative* values and thus a *stable* molecule ion. Why are they more successful than the early attempts, in the 1920s, by Pauli,<sup>4</sup> and independently Niessen,<sup>20</sup> with the Sommerfeld quantization conditions of the old quantum theory?

For the same reason that Sommerfeld had excluded the angular quantum number  $l = 0$  for the  $H$  atom—avoidance of electron collision with the nucleus—both Pauli and Niessen excluded electron motion in the nuclear plane of the  $H_2^+$  molecule ion. They then found the lowest admissible quantum state to be  $(n_\xi, n_\eta, n_\varphi) = (0, 1, 1)$ , denoted  $2p\Pi_u$  in molecular spec-

troscopy, with  $E_0(P, N) = -0.52 R_y$  at  $R_0(P, N) = 5.53 \pm 0.01 r_B$ , depicted by the triangle in the top part of Fig. 7. The QM energy<sup>21</sup> of that quantum state is  $E_0(2p\Pi_u) = -0.27 R_y$  at  $R_0(2p\Pi_u) \approx 8 r_B$ , marked by the solid dot at the minimum of the dotted curve. Since both these energy values are higher than the ground state of a free hydrogen atom, they give rise to *positive* molecular binding energies and thus to spontaneous dissociation,  $H_2^+(2p\Pi_u) \rightarrow H + H^+$ . Qualitatively, Pauli’s and Niessen’s finding of energetic *instability* is borne out by quantum mechanics for this excited state of  $H_2^+$  (Pauli’s argument<sup>4</sup> about “dynamical stability” notwithstanding). The deviation of their historical value ( $\Delta$ ) from the (dotted) QM curve is remarkably small—comparable to those of the CO and SR results for the ground state. Pauli’s and Niessen’s misfortune, though, was that they *misinterpreted* their result as the molecule ion’s ground state—an assessment with fateful consequences in the development of quantum theory.

### C. Discussion

Why do the semiclassical results of the Coulomb oscillator and of SR’s quantization deviate from the QM solution of the  $H_2^+$  molecule ion? Strand and Reinhardt explain the deviation of their primitive quantization from QM with effective potential barriers arising from constrictions due to conservation of both the energy  $E$  and the bifocal Runge-Lenz component  $\Omega_c$  (the angular momentum vanishes for the ground state,  $\mathbf{M} = 0$ ). The most drastic consequence of those barriers is the discontinuity of  $E_{el}$  at  $R^*$  (see Fig. 7) and the large deviations at closer proton separation,  $R < R^*$ . While the simulation of quantum mechanical tunneling beyond the semiclassical turning points of librations is adequately achieved by EKB quantization under the isotropic symmetry of a free  $H$  atom,<sup>19</sup> Eq. (19) is less successful under the lower symmetry of  $H_2^+$ . When SR remedy the situation with “unified” semiclassical quantization conditions, then  $E_{el}$  agrees, for all practical purposes, with QM. Those unified quantization conditions, going well beyond Eq. (19), are sophisticated in their dependence on  $E_{el}$ ,  $\Omega_c$ , and the hyperbolic turning points  $\eta_{\pm}$ . They will not be discussed here.

The reason for the deviation of the CO results from the QM values is the *neglect* of the electron’s *wave* nature in the underlying quantization condition, Eq. (16). In proposing his wave hypothesis de Broglie<sup>22</sup> already showed that the quantization condition of the Bohr model,  $A_n = nh$ , is equivalent

to  $n$  standing waves along the  $n$ th Bohr orbit. If  $s$  denotes the position along the Bohr orbit, then the de Broglie wave can be expressed as  $w(s) = \sin[2\pi a_n(s)/h]$ , with the variable  $a_n(s) = (A_n/S_n) \int_0^s ds'$  along the orbit's circumference  $S_n = 2\pi r_n$ . A generalization gives for the Coulomb oscillator of a free  $H$  atom in the ground state ( $n = 1$ ), its de Broglie wave as

$$w(z) = \sin[2\pi a(z)/h] \quad (20a)$$

with

$$a(z) = m \int_0^z v(z') dz' \quad (20b)$$

and the speed  $v(z')$  from Eq. (2). This de Broglie wave, shown by the line curve in Fig. 8 for a free  $H$  atom positioned at  $+c$ , has a node at the nucleus and at each turning point. By the above characterization, those turning points are “soft,” and it is their softness that ensures the exact energy of the free atom. However, when Eq. (20ab) is applied to  $H_2^+$  for proton separations beyond the bifurcation value,  $R > \check{R}$ , with axial speed from Eq. (8ab) and integration away from the occupied nucleus,  $\int_c^z \dots$ , then the de Broglie wave is found to be “truncated” (no nodes) at both the outer and inner turning point (see Fig. 8, small circles). Those turning points are “hard” and give rise to incorrect energies. Qualitatively, an augmentation of the truncated de Broglie wave with (exponential) “tunneling tails,” determined by the negative kinetic energy in the classically “forbidden” region, would “soften” the turning points. This would give rise to an *effective* far turning point farther out,  $C_{eff} > C$ , and accordingly raise the CO energy, Eq. (7), toward the QM result.

When the proton separation is below bifurcation,  $R < \check{R}$ , then Eq. (20b) should be integrated from the midpoint 0 in both the axial and lateral direction rather than favoring one nucleus with the node of the de Broglie wave. Again, the de Broglie wave is found to be truncated at the axial and lateral turning points,  $C$  and  $B$ , respectively (see Fig. 9). An exception exists for the proton separation  $R^*$ . The de Broglie wave, shown in Fig. 10, then has a minimum at both turning points,  $w(C) = w(B) = -1$ , according to action values of  $A_z = \frac{3}{4}h$  and  $A_y = \frac{1}{4}h$ . Such turning points seem to be “benign”—reminiscent of the soft turning points in the free-atom case—and cause the CO energy  $E_{el}(R^*)$  in Fig. 7 to be *exact*. At still smaller proton separation,  $R < R^*$ , the de Broglie wave is truncated again (not shown). The limit  $R = 0$  corresponds to a Coulomb oscillator in the free  $He^+$  ion which, like in the

free  $H$  atom for  $R = \infty$ , has de Broglie nodes at the turning points and an exact energy value.

If the explanation that the CO energy  $E_{el}(R)$  deviates from the QM curve because of the *neglect of wave effects* is valid, then this sheds new light on the SR results. The opposite sign of the CO and SR deviations then suggests that SR's primitive EBK quantization, while appropriate for a free atom, simulates *too much wave effects* under the lower symmetry of the  $H_2^+$  molecule ion. However, the *average* of both those semiclassical quantizations seems to be an excellent compromise, as evidenced by the close agreement of the corresponding total energy ( $\diamond$ ) with the (dashed) QM curve in Fig. 7.

In conclusion, semiclassical quantization can rise to Gutzwiller's challenge and "explain" the chemical bond in the paradigm molecule,<sup>23</sup>  $H_2^+$ , by a combination of classical mechanics, quantization, and moderate wave effects.

## IV. ACKNOWLEDGMENTS

I thank Duane Siemens and Ernst Mohler for valuable discussions. Many thanks to Preston Jones for help with computer integration and graphics. I also thank Professor Gutzwiller for advice and his kind encouragement.

## V. APPENDIX A: QUANTIZATION

By Eq. (4) the action integral of the atomic Coulomb oscillator is

$$A = \frac{1}{\phi} \oint p_z dz = -\frac{4e}{\phi} \sqrt{2Zm} \int_{\Gamma}^0 \sqrt{\frac{1}{z} - \frac{1}{\Gamma}} dz. \quad (4')$$

For a comparison with integral tables we change notation to  $x = z$  and use the abbreviation  $a = -1/\Gamma$ . Then

$$\int \sqrt{\frac{1}{z} - \frac{1}{\Gamma}} dz = \int \sqrt{\frac{1}{x} + ax} dx = \int \frac{\sqrt{X}}{x} dx \quad (21)$$

with  $X = ax^2 + x$ . Integration tables give

$$\int \frac{\sqrt{X}}{x} dx = \sqrt{X} + \frac{1}{2} \int \frac{dx}{\sqrt{X}}. \quad (22)$$



The first term on the rhs, evaluated at the limits of the  $\int_{\Gamma}^0$  integration, vanishes. The last integral in Eq. (22), tabulated as

$$\int \frac{dx}{\sqrt{X}} = (-\sqrt{\Gamma}) \arcsin(1 - 2x/\Gamma), \quad (23)$$

and evaluated at the limits,  $x = 0$  and  $x = \Gamma$ , contributes

$$- [\arcsin(1) - \arcsin(-1)]\sqrt{\Gamma} = -\pi\sqrt{\Gamma}. \quad (24)$$

Combining Eqs. (4'), (22) and (24), together with a fold-out factor  $\phi = 2$ , gives the action integral, to be equated with the Sommerfeld quantization condition,

$$A_n = -\frac{4e}{\phi} \sqrt{2Zm} \frac{1}{2} (-\pi\sqrt{\Gamma}) = nh. \quad (25)$$

We square Eq. (25) and solve for the amplitude of the quantized Coulomb oscillator,

$$\Gamma_n = 2 \frac{r_B}{Z} n^2, \quad (26)$$

in terms of the Bohr radius  $r_B$ .

## VI. APPENDIX B: DATA

TABLE I. Electronic ground-state energy  $E_{el}$  for various nuclear separations  $R$  of the  $H_2^+$  molecule from quantum-mechanical calculations (QM, Ref 21), the ‘‘primitive’’ semiclassical quantization of Strand and Reinhardt (SR, Ref. 15), and the present Coulomb-oscillator approach (CO).

R ( <i>a.u.</i> )	QM ( $R_y$ )	SR ( $R_y$ )	CO ( $R_y$ )
0.00	-4.00	-4.00	-4.00
0.25	-3.80	-4.75	-3.35
0.50	-3.47	-4.27	-3.12
0.75	-3.11	-3.76	-2.93
1.00	-2.90	-3.34	-2.81
1.25	-2.68	-3.07	-2.67
1.50	-2.50	-2.19	-2.55
1.75	-2.34	-2.09	-2.45
2.00	-2.21	-1.99	-2.36
2.50	-1.99	-1.79	-2.18
3.00	-1.82	-1.66	-2.02
3.50	-1.69	-1.56	-1.87
4.00	-1.59	-1.49	-1.75
5.00	-1.45	-1.40	-1.54
6.00	-1.36	-1.33	-1.38
8.00	-1.26	-1.25	-1.27
10.00	-1.20	-1.20	-1.20
12.00	-1.17	-1.17	-1.17

## References

- <sup>1</sup>Other failures were its inability to give the brightness of spectral lines and the unsuccessful extension to the *He* atom.
- <sup>2</sup>M. Jammer, *The Conceptual Development of Quantum Mechanics* (McGraw-Hill, New York, 1966), p. 129.
- <sup>3</sup>Instead of the traditional notation  $k$  for the angular quantum number in the old quantum theory, we will use the letter  $l$  ( $= k$ ) to facilitate the connection with quantum mechanics.
- <sup>4</sup>W. Pauli, “Über das Modell des Wasserstoffmolekülions,” *Annalen der Physik* **68**, 177-240 (1922). A history of Pauli’s thesis is given by C. P. Enz, “No Time to be Brief: A Scientific Biography of Wolfgang Pauli” (Oxford UP, 2002), pp. 63-74.
- <sup>5</sup>M. C. Gutzwiller, *Chaos in Classical and Quantum Mechanics* (Springer, New York, 1990), p. 36.
- <sup>6</sup>A. Sommerfeld, “Zur Quantentheorie der Spektrallinien,” *Annalen der Physik*, **51**, 1-94 (1916).
- <sup>7</sup>This length of semiminor axis has been modified from Sommerfeld’s original expression,  $b_{nl} = (r_B/Z)nk$ , to achieve agreement with expressions from quantum mechanics.
- <sup>8</sup>If the nuclear charge is uniformly distributed, then  $Z'(r) = (r/r_N)^3Z$ , and the electron’s motion inside the nucleus is harmonic.
- <sup>9</sup>M. Bucher, D. Elm and D. P. Siemens, “Average position in Kepler motion,” *Am. J. Phys.* **66**, 929-930 (1998).
- <sup>10</sup>L. Pauling and E. B. Wilson, *Introduction to Quantum Mechanics* (Dover, New York, 1935) p. 144.
- <sup>11</sup>Although almost all quantum texts use the weaker statement “at the nucleus.”
- <sup>12</sup>M. Bucher, “The electron inside the nucleus: An almost classical derivation of isotropic hyperfine interaction,” *Eur. J. Phys.* **21**, 19-22 (2000).

- <sup>13</sup>A. Einstein, “*Zum Quantenansatz von Sommerfeld und Epstein*,” Verh. Dtsch. Phys. Ges. **19**, 82-92 (1917). A summary with modern comments is given by A. D. Stone, “*Einstein’s unknown insight and the problem of quantizing chaos*,” Phys. Today, Aug. 2005, pp. 37-43.
- <sup>14</sup>Eq. (3), introduced as Sommerfeld quantization for familiarity’s sake, is also an Einstein quantization condition.
- <sup>15</sup>M. P. Strand and W. P. Reinhardt, “*Semiclassical quantization of the low lying electronic states of  $H_2^+$* ,” J. Chem. Phys. **70**, 3812-27 (1979).
- <sup>16</sup>The (one-center) Runge-Lenz vector,  $\mathbf{\Omega} = \mathbf{v} \times \mathbf{L} - Ze^2\mathbf{r}/r$ , of a Sommerfeld orbit of angular momentum  $\mathbf{L}$  has a magnitude proportional to the ellipse’s eccentricity  $\varepsilon$  and points from the nucleus toward the perihelion; see J. Morehead, “*Visualizing the extra symmetry of the Kepler problem*,” Am. J. Phys. **73**, 234-239 (2005). For a Coulomb oscillator ( $L = 0$ ,  $\varepsilon = 1$ ),  $\mathbf{\Omega}$  oscillates and thus is *not conserved*. Neither is  $\Omega_c$  of the two-center *Coulomb oscillator* conserved; see H. A. Erikson and E. L. Hill, “*A Note on the one-electron state of diatomic molecules*,” Phys. Rev. **75**, 29-31 (1949); and also C. A. Coulson and A. Joseph, “*A constant of the motion for the two-center Kepler problem*,” Int. J. Quantum Chem. **1**, 337-347 (1967).
- <sup>17</sup>The trajectory will eventually revisit an arbitrarily close neighborhood of any previous point.
- <sup>18</sup>Ref. 5, pp. 207-215.
- <sup>19</sup>L. J. Curtis and D. G. Ellis, “*Use of the Einstein-Brillouin-Keller action quantization*,” Am. J. Phys. **72**, 1521-1523 (2004).
- <sup>20</sup>K. F. Niessen, “*Zur Quantentheorie des Wasserstoffmoleküllions*,” Annalen der Physik **70**, 129-134 (1923).
- <sup>21</sup>M. M. Madsen and J. M. Peek, At. Data **2**, 171 (1971); E. Teller and H. L. Sehlin, in *Physical Chemistry, An Advanced Treatise* (Academic, New York, 1970), Vol. **5**, p. 35.
- <sup>22</sup>L. de Broglie, “*Ondes et quanta*,” Comptes Rendus **177**, 507-510 (1923).
- <sup>23</sup>K. Ruedenberg, “*The physical nature of the chemical bond*,” Rev. Mod. Phys. **34**, 326-276 (1962).

## VII. FIGURE CAPTIONS

Fig. 1. Partial trajectory of an extranuclear orbit  $XX'$  and of a penetrating orbit  $PP'$  through nucleus  $N$ . The dotted line  $S$  shows the major symmetry axis of  $XX'$ .

Fig. 2. Line orbit of a Coulomb oscillator with nucleus at origin 0 and turning points at  $\pm\Gamma$ .

Fig. 3. Axial electron speed  $v$  vs. position  $z$  of an electron in Coulomb oscillation for the ground state,  $n = 1$ , of a hydrogen atom  $H$  ( $Z = 1$ , solid curve) and a helium ion  $He^+$  ( $Z = 2$ , dashed curve). The area under one wing of each curve represents the radial action,  $A = 1h$ .

Fig. 4. Axial Coulomb oscillation in an  $H_2^+$  molecule ion between axial turning points  $\pm C$  and through nuclei at  $\pm c$ ; perpendicular oscillation between lateral turning points  $\pm B$  and through midpoint 0.

Fig. 5. Axial speed  $v$  vs. position  $z$  in the ground state of an  $H_2^+$  molecule ion (bold curve) and, for comparison, of a free  $H$  atom (thin curve). Circles indicate the axial the positions of the nuclei, here with a *large* separation,  $R = 6 r_B$ .

Fig. 6. Axial speed  $v$  vs. position  $z$  in the ground state of an  $H_2^+$  molecule ion (M-shaped bold curve) and, for comparison, of a free  $H$  atom ( $\Lambda$ -shaped thin curve, centered at the right nucleus). The  $\cap$ -shaped dotted curve, centered at 0, shows the lateral speed  $u$  vs. the perpendicular position  $y$  in the molecule. Circles indicate the axial positions of the nuclei, here with a *small* separation,  $R = 2 r_B$ .

Fig. 7. Dependence of energies of  $H_2^+$  on internuclear distance  $R$ . *Bottom*: Electronic energy  $E_{el}$  from quantum mechanics (QM, solid curve), primitive semiclassical quantization by Strand and Reinhardt (SR,  $\circ$ ) and the present Coulomb-oscillator approach (CO,  $+$ ). *Middle*: Total energy  $E$  of the  $1s\Sigma_g$  ground state from QM (dashed curve) with minimum ( $\bullet$ ), values by SR ( $\square$ ) and CO ( $\times$ ) and their average ( $\diamond$ ), energy of a free  $H$  atom (dashed horizontal line). *Top*: Total energy  $E$  of the  $2p\Pi_u$  state from QM (dotted curve) with minimum ( $\bullet$ ), and historical value by Pauli and Niessen ( $\triangle$ ).

Fig. 8. de Broglie wave of the free  $H$  atom Coulomb oscillator (curve) and of the  $H_2^+$  Coulomb oscillator (small circles) for the same proton separation as in Fig. 5,  $R = 6 r_B$ . Large circles indicate the axial positions of the nuclei.

Fig. 9. de Broglie wave of the  $H_2^+$  Coulomb oscillator along axial distance  $OC$  from Fig. 4 (right side of graph) and lateral distance  $OB$  (left side).

Large circles indicate the axial positions of the nuclei, here with the same separation as in Fig. 6,  $R = 2 r_B$ .

Fig. 10. Same as Fig. 9 but for the proton separation  $R^* = 1.38 r_B$  where the semiclassical energy is exact.

2-24-2006

# Coulomb oscillation in the hydrogen atom and molecule ion

Manfred Bucher

Physics Department, California State University, Fresno  
Fresno, California 93740-8031

## Abstract

Semiclassical oscillation of the electron through the nucleus of the  $H$  atom yields both the exact energy and the correct orbital angular momentum for  $l = 0$  quantum states. Similarly, electron oscillation through the nuclei of  $H_2^+$  accounts for a stable molecule ion with energy close to the quantum mechanical solution. The small discrepancy arises from the neglect of the electron's wave nature.

PACS numbers: 03.65.Sq, 31.10.+z, 31.20.Pv

## I. INTRODUCTION

Two of the reasons why the old quantum theory of Bohr and Sommerfeld was abandoned in the mid 1920s were the theory's failure to give the correct multiplet structure of the hydrogen atom and the stability of the hydrogen molecule ion,  $H_2^+$ .<sup>1</sup> The old vector model of angular momentum<sup>2</sup> gave, for a given principal quantum number  $n$ , sublevels with angular quantum numbers  $l = 1, 2, \dots, n$ .<sup>3</sup> Spectroscopic evidence, however, showed multiplicities of spectral line splitting in a magnetic field according to  $l = 0, 1, \dots, n - 1$ . Max Jammer, in his review,<sup>2</sup> notes that “the old quantum theory could never resolve this inconsistency.”

A treatment of the hydrogen molecule ion with Sommerfeld's quantization conditions had been Wolfgang Pauli's doctoral thesis of 1922.<sup>4</sup> Pauli found its molecular binding energy to be positive (non-binding)—contrary to (later) experimental findings. Martin Gutzwiller<sup>5</sup> thinks that “the solution of this problem can be rated, with only slight exaggeration, as the most important in quantum mechanics, because if an energy level with a [more] negative value [than of a free hydrogen atom] can be found, then the chemical bond between two protons by a single electron has been explained.”

Both dilemmas of the old quantum theory can be resolved, though, with a single extension: an oscillation of the electron through the nucleus (nuclei) of the atom (molecule). In essence this solution is already formally included in Sommerfeld's theory of the hydrogen atom<sup>6</sup> but was explicitly omitted by Sommerfeld and his school as being *unphysical*. The case in point, obtained with Sommerfeld's quantization conditions for radial and angular motion, is a quantum state with zero angular action, characterized by an angular quantum number  $l = 0$ . What is its orbit?

The geometry of an  $nl$  Sommerfeld ellipse is given by its semimajor axis,  $a_{nl} = (r_B/Z)n^2$ , and semiminor axis,  $b_{nl} = (r_B/Z)n\sqrt{l(l+1)}$ .<sup>7</sup> Here  $r_B = h^2/4\pi^2me^2$  is the Bohr radius in terms of fundamental constants, serving as an atomic distance unit, and  $Ze$  is the nuclear charge. An  $(n, 0)$  orbit is thus a line ellipse with its nuclear focus at one end and its empty focus at the other. This case was regarded as unphysical because of the electron's collision with the nucleus—an uncritical adaptation from celestial mechanics. A closer inspection confirms that a line ellipse with *terminal* nuclear focus is indeed unphysical—but for quite a different reason!

Figure 1 Here



Fig. 1. Partial trajectory of an extranuclear orbit  $XX'$  and of a penetrating orbit  $PP'$  through nucleus  $N$ . The dotted line  $S$  shows the major symmetry axis of  $XX'$ .

Leaving quantization conditions momentarily aside, what would happen if we *continuously* decrease an angular quantum number  $\lambda$  while keeping the principal quantum number  $n$  constant? We then would get more and more slender ellipses with the same length of major axis,  $2a_n$ . By basic electric theory, the nuclear Coulomb potential outside a *finite-size* nucleus  $N$  is given by the point potential as if all nuclear charge,  $+Ze$ , was concentrated at the center of the nucleus. This holds as long as the electron orbit stays outside the nucleus. Two borderline cases are illustrated in Fig. 1. For a very small  $\lambda$  value, say  $0 < \lambda_X \ll 1$ , we obtain a very slender elliptical orbit with partial trajectory  $XX'$  about the nucleus. Further decrease of  $\lambda$  to  $\lambda_P < \lambda_X$  causes an intrusion of the electron into the finite nucleus of radius  $r_N$  (see trajectory  $PN$  in Fig. 1). Once inside, at a distance  $r < r_N$  from the center, then, by Gauss's law, only a fraction of the nuclear charge,  $Z'(r)e < Ze$ , acts on the electron via centripetal force.<sup>8</sup> Accordingly, the electron's exit trajectory  $NP'$  is no longer symmetric to its approach trajectory  $PN$  with respect to the major axis  $S$  of the (partial) ellipse  $XX'$ . In the extreme case of a head-on penetration of the nucleus,  $\lambda = 0$ , there is no centripetal force at all! The electron will then, with almost constant speed, traverse the nucleus, continue, with decreasing speed, to the opposite turning point of its line orbit and revert its motion periodically. We want to call the electron's straight-line oscillation in the Coulomb potential of a finite-size nucleus a "*Coulomb oscillator*."

## II. HYDROGEN ATOM

For the formal treatment of the non-relativistic Coulomb oscillator we designate the  $z$  axis along the line orbit, with turning points at  $z = \pm\Gamma$  and nuclear position at  $z = 0$  (see Fig. 2). The electron's total energy  $E$  at position  $z$  must equal the potential energy at a turning point,

$$E = \frac{1}{2}mv^2 - \frac{Ze^2}{|z|} = -\frac{Ze^2}{\Gamma}. \quad (1)$$

This gives the electron's speed along the  $z$  axis,

$$v = \pm e \sqrt{\frac{2Z}{m}} \sqrt{\frac{1}{|z|} - \frac{1}{\Gamma}}. \quad (2)$$

Figure 3 displays its dependence on the axial position as a two-wing curve cusped at the nucleus. Atomic units (*a.u.*) are used, that is, the Bohr radius  $r_B$  and the “Bohr speed”  $v_B = 2\pi e^2/h = \alpha c$ —the electron speed in the ground-state Bohr orbit of the  $H$  atom—with fine-structure constant  $\alpha \approx 1/137$  and speed of light  $c$ . The curve’s wing along the positive  $z$  axis,  $|z| = r$ , gives the *radial* speed,  $v_r(r) = |v(z)|$ , necessary for Sommerfeld’s *radial* quantization condition,

$$\oint p_r dr = m \oint v_r(r) dr = n_r h. \quad (3)$$

Here  $p_r$  is the radial momentum,  $n_r = 1, 2, \dots$  is the radial quantum number, and  $h$  is Planck’s quantum of action. Integration is over one period of the radial motion,  $z = +\Gamma \rightarrow 0 \rightarrow +\Gamma$ . Graphically, the radial quantization is illustrated in Fig. 3 by the area under *one* wing of the speed curve. For a line orbit,  $l = 0$ , the radial quantum number equals the principal quantum number,  $n \equiv n_r + l = n_r$ .

In order to express the radial quantization in terms of *axial* motion we employ a “fold-out factor,”  $\phi = 2$ , to compensate for the doubling of integration range in the extension from the radial one-wing speed curve to the axial two-wing curve. The quantization is thus restated,

$$\frac{1}{\phi} \oint p_z dz = \frac{m}{\phi} \oint v(z) dz = n_z h, \quad (3')$$

with axial quantum number  $n_z = n_r = n$  and integration over the axial double-wing range,  $z = +\Gamma \rightarrow -\Gamma \rightarrow +\Gamma$ . By symmetry we can restrict the axial action integral to one quarter of the oscillation, say  $z = +\Gamma \rightarrow 0$ ,

$$\frac{1}{\phi} \oint p_z dz = -\frac{4m}{\phi} \int_{\Gamma}^0 v(z) dz = -\frac{4e}{\phi} \sqrt{2Zm} \int_{\Gamma}^0 \sqrt{\frac{1}{z} - \frac{1}{\Gamma}} dz = nh. \quad (4)$$

Here the electron’s motion in the negative  $z$  direction is accounted for by the negative sign. Although the electron’s speed through a point nucleus diverges,  $v(0) = \infty$ , the action integral, Eq. (4), stays finite and determines

the quantized amplitude  $\Gamma_n$  of the Coulomb oscillator. Graphically the amplitude  $\Gamma_n$  must be such that it stretches the speed curve horizontally to the extent that the area under one wing,  $A_n = nh$ , represents the quantized action. The analytic solution, derived in Appendix A, is

$$\Gamma_n = 2\frac{r_B}{Z}n^2. \quad (5)$$

Inserting Eq. (5) into Eq. (1) yields the quantized energy,

$$E_n = -\frac{Z^2e^2}{\Gamma_n} = -\frac{Z^2}{n^2}R_y, \quad (6)$$

in terms of the Rydberg energy unit,  $R_y = 2\pi^2me^4/h^2 = 13.6 \text{ eV}$ , and in agreement with the energy of the  $n$ th Bohr orbit.

Note that Eq. (5) gives the amplitude of the  $n$ th Coulomb oscillator as *twice* the radius of the  $n$ th Bohr orbit or of the semimajor axis of an  $nl$  Sommerfeld ellipse,  $r_n = a_{nl} = (r_B/Z)n^2$ . For comparison, the time-average radial distance of a Kepler orbit<sup>9</sup> of major and minor semiaxes  $a$  and  $b$ , respectively, is  $\langle r \rangle_t = (3a^2 - b^2)/(2a)$ . A line ellipse ( $b = 0$ ) has then  $\langle r \rangle_t = \frac{3}{2}a$ . Applied to an  $nl$  Sommerfeld orbit,<sup>9</sup> its average size,  $\langle r_{nl} \rangle_t = (r_B/Z)[3n^2 - l(l + 1)]/2$ , is in agreement with the corresponding quantity from quantum mechanics,<sup>10</sup>  $\langle r_{nl} \rangle = \int \psi^* r \psi d^3r$ . Thus the time-average radial distance of a Coulomb oscillator is  $\langle r_{n0} \rangle_t = \frac{3}{2}(r_B/Z)n^2$ . For the ground state of the hydrogen atom,  $n = 1$ , this gives  $\langle r_{10} \rangle_t = \frac{3}{2}r_B$ , as is well-known from quantum mechanics.<sup>10</sup>

The concept of the electron's semiclassical Coulomb oscillation is consistent with the Fermi-contact term of hyperfine interaction for  $l = 0$  states, which arises from the presence of the electron *inside* the nucleus. This is familiar from quantum mechanics<sup>11</sup> and can be interpreted semiclassically as a local-field effect.<sup>12</sup>

To be sure, the extension of Sommerfeld's theory by the Coulomb oscillator resolves the discrepancy of the old quantum theory with spectroscopy, mentioned above, only at the *low* end of angular quantum numbers,  $l = 0$ . The resolution at the high end—repeal of the circular Bohr orbit,  $l \neq n$ —involves an analysis in terms of space quantization which is beyond the scope of the present study.

### III. HYDROGEN MOLECULE ION

#### A. Formalism

A hydrogen molecule ion,  $H_2^+$ , consists of two proton nuclei and one electron. We assume, in adiabatic approximation, the protons located at fixed positions  $z = \pm c$  on the molecular axis (see Fig. 4). The term ‘‘Coulomb oscillator’’ denominates again the motion of a point electron, now along either the line through the protons ( $z$  axis) and with turning points  $\pm C$ , or along the perpendicular line through the midpoint ( $y$  axis) with turning points  $\pm B$ . The molecule ion’s total energy  $E$  at any position on the axis,  $-C \leq z \leq +C$ , must equal the potential energy at the turning point  $C$ ,

$$E = \frac{1}{2}mv^2 - \frac{e^2}{|z+c|} - \frac{e^2}{|z-c|} + \frac{e^2}{2c} = -\frac{e^2}{C+c} - \frac{e^2}{C-c} + \frac{e^2}{2c}. \quad (7)$$

For electron positions beyond the protons,  $z > c$ , this gives an electron speed

$$v_{out} = \pm \frac{2e}{\sqrt{m}} \sqrt{\frac{z}{z^2 - c^2} - \frac{C}{C^2 - c^2}}. \quad (8a)$$

For positions between the protons,  $0 < z < c$ , the corresponding speed is

$$v_{in} = \pm \frac{2e}{\sqrt{m}} \sqrt{\frac{c}{c^2 - z^2} - \frac{C}{C^2 - c^2}}. \quad (8b)$$

The speed expressions will be used in the action integral,

$$\frac{1}{\phi} \oint p_z dz = \frac{2m}{\phi} \int_C^{-C} v(z) dz = A_z = A_{out} + A_{in}, \quad (9)$$

with outer contribution

$$A_{out} = \frac{2m}{\phi} \left[ \int_C^c v_{out}(z) dz + \int_{-c}^{-C} v_{out}(z) dz \right] \quad (10a)$$

and inner contribution

$$A_{in} = \frac{2m}{\phi} \int_c^{-c} v_{in}(z) dz. \quad (10b)$$

Here  $\phi$  is a fold-out factor to be specified below.

If the conditions are such that the electron swings along the  $z$  axis through the midpoint 0, that is,  $v_{in}(0) > 0$ , then there exists also an oscillation along the  $y$  axis with lateral speed  $u$ , having the same total energy,

$$E = \frac{1}{2}mu^2 - \frac{2e^2}{\sqrt{y^2 + c^2}} + \frac{e^2}{2c} = -\frac{2e^2}{\sqrt{B^2 + c^2}} + \frac{e^2}{2c}. \quad (11)$$

Equal energy at the axial and lateral turning points,  $E(C) = E(B)$ , Eqs. (7) and (11), determines the latters' geometric dependence,

$$B = \sqrt{C^2 + \frac{c^4}{C^2} - 3c^2}. \quad (12)$$

Solving Eq. (11) for the lateral speed,

$$u = \pm \frac{2e}{\sqrt{m}} \sqrt{\frac{1}{\sqrt{y^2 + c^2}} - \frac{1}{\sqrt{B^2 + c^2}}}, \quad (13)$$

provides the integrand of the action integral over a lateral oscillation,

$$A_y = \frac{1}{\phi} \oint p_y dy = \frac{2m}{\phi} \int_B^{-B} u(y) dy. \quad (14)$$

Subtraction of the protons' mutual repulsion from the total energy  $E$  of axial or lateral motion, Eqs. (7) and (11), gives the *electronic* energy,

$$E_{el} = E - \frac{e^2}{R}, \quad (15)$$

in its dependence on the proton separation,  $R = 2c$ . This brackets the molecular problem with known atomic results, Eq. (6), in the limits of  $R = \infty$  (free  $H$  atom,  $Z = 1$ ) and  $R = 0$  (free  $He^+$  ion,  $Z = 2$ ). For those cases, as well as any proton-proton distance  $R$  between, we keep the action constant,

$$A = A_z + A_y = nh. \quad (16)$$

Equation (16) is the *Einstein* quantization condition<sup>13</sup>—a generalization of Sommerfeld's quantization over separable variables—where the *quantum sum* equals the sum of action integrals over topologically independent paths in phase space.<sup>14</sup>

Here we treat the molecule ion only in its *ground state*,  $n = 1$ . Analytic solutions of the action integrals, Eqs. (10ab) and (14), are complicated due to elliptic functions. We therefore integrate numerically and visualize the integrals by the area under the corresponding speed curves. The bold curve in Fig. 5 shows the axial electron speed  $v(z)$  for a *far* proton separation,  $R = 6 r_B$ . The electron, in its semiclassical motion, then oscillates only about (and through) the right proton. The area under the speed curve, Eq. (8ab), proportionally represents the ground state's unity of action,  $m \oint v(z) dz = \phi h$ , with a fold-out factor  $\phi = 2$  in analogy to the free-atom case, Eq. (4). The thin curve shows, for comparison, the axial electron speed in a free  $H$  atom—familiar from Fig. 3—centered at the same proton position,  $+c$ . The pull from the left proton (at  $-c$ ) on the oscillating electron can be seen by the distortion of the speed function  $v(z)$  and the redistribution of the area under the curve.

When, with closer proton separation  $R$ , as in Fig. 6, the electron swings past the midpoint 0, then the single-cusp speed curve  $v(z)$  from Fig. 5—akin in shape to letter  $\Lambda$ —becomes double-cusped (akin to letter M) and symmetric with respect to the bisector ( $y$  axis). Now there is also a lateral oscillation with speed  $u(y)$  having the same total energy  $E$ . The equality of  $E$  in both cases can be seen in Fig. 6 by the equality of axial and lateral speed at the midpoint,  $v(0) = u(0)$ —a position where the electron experiences the same potential in either case. For convenience the lateral speed  $u(y)$ , though perpendicular to the proton axis, is displayed in Fig. 6 together with the axial speed  $v(z)$ . The lateral speed curve  $u(y)$ , drawn dotted, is readily recognized by its dome shape ( $\cap$ ). At the bifurcation value of the proton separation,  $\check{R}$ , where the electron starts swinging though the midpoint 0, the axial speed curve  $v(z)$  changes from its one-centered  $\Lambda$  shape to a two-centered M shape. The *area* under the axial speed curve then abruptly doubles,  $M(\check{R} - \delta) \approx 2\Lambda(\check{R} + \delta)$ , upon a very small change in proton separation,  $\delta \ll \check{R}$ . In order to keep the action integral continuous at  $\check{R}$ , the sudden area doubling is compensated by a corresponding doubling of the fold-out factor from  $\phi = 2$  for  $R > \check{R}$  to  $\phi = 4$  for  $R < \check{R}$ . The same fold-out factor,  $\phi = 4$ , must be used for the lateral action integral  $A_y$ , Eq. (14), as will become clear shortly.

The unity of action,  $A = 1h$ , is visualized again in Fig. 6. To this end we compare the right half of the bold M-shape curve of axial electron speed in the molecule with the thin curve  $\Lambda(H)$  of the axial speed in a free  $H$  atom positioned at the right nucleus,  $+c$ . Due to attraction from the left nucleus,

the right wing of the M curve is smaller than that of  $\Lambda(H)$  by the area of lobe  $L$ . On the other hand, the left flank of the  $\Lambda(H)$  curve that extends over the negative  $z$  axis is smaller than the left wing of the lateral speed curve  $\cap$  by the area of slice  $S$ . The area under the free-atom curve is then

$$\Lambda(H) \approx \frac{1}{2}M + L + \frac{1}{2}\cap - S. \quad (17a)$$

The areas of lobe and slice are comparable,

$$L \approx S. \quad (17b)$$

When the tiny notch to the right of the saddle point of M is taken into account, then the approximations (17ab) become equations and combine to

$$M + \cap = 2\Lambda(H). \quad (18)$$

The area under both the axial and lateral speed curves is thus four times the area under *one* wing of the free-atom curve,  $M + \cap = 4 \times \frac{1}{2}\Lambda(H)$ . Since the latter represents one quantum of action,  $h$ , the combined area  $M + \cap$  visualizes its *double* fold-out,  $\phi = 4$ .

With very close proximity of the nuclei,  $R \rightarrow 0$ , the crests of the M curve start merging while its saddle point,  $v(0)$ , keeps rising. In the  $R = 0$  limit of fusing nuclei the axial electron speed becomes that of a free  $He^+$  ion,  $M \rightarrow \Lambda(He^+)$ , familiar from Fig. 3. Concurrently, the lateral speed curve  $\cap$  rises at its peak,  $u(0) = v(0)$ , and narrows at its base until it, too, turns into the speed curve of the free  $He^+$  ion,  $\cap \rightarrow \Lambda(He^+)$ . In the  $R = 0$  limit the three curves merge,  $M(0) = \cap(0) = \Lambda(He^+)$ .

The results of the Coulomb-oscillator approach will be compared with another semiclassical calculation of  $H_2^+$ , by Strand and Reinhardt.<sup>15</sup> These authors, like Pauli,<sup>4</sup> separate the equation of motion in spheroidal coordinates,  $\xi = (r_+ + r_-)/2c$ ,  $\eta = (r_+ - r_-)/2c$  and  $\varphi$  by virtue of the constants of the motion: total energy  $E$ , angular momentum  $\mathbf{M}$  about the  $z$  axis, and a component of the bifocal Runge-Lenz vector,  $\Omega_c$ .<sup>16</sup> Here  $r_+$  ( $r_-$ ) is the distance of the electron from the nucleus at  $+c$  ( $-c$ ). Strand and Reinhardt (SR) solve the ensuing one-dimensional differential equations with classical Poisson-bracket techniques. They find the electron's trajectories conditionally periodic<sup>17</sup> and regionally confined due to restrictions from  $E$ ,  $\mathbf{M}$  and  $\Omega_c$ . However, unlike Pauli, who used Sommerfeld quantization, SR employ the Einstein-Brillouin-Keller (EBK) quantization conditions,

$$A_j = \oint p_j dj = (n_j + \frac{1}{2})h, \quad j = \xi, \eta \quad (19ab)$$

and

$$A_\varphi = \oint p_\varphi d\varphi = n_\varphi h. \quad (19c)$$

The background of EBK quantization touches on the foundations of classical and quantum mechanics.<sup>18</sup> For the present purpose its essential rationale may be summarized as follows: A semiclassical treatment involves turning points of radial, or other librating motion. Any tunneling through “forbidden” regions of negative kinetic energy is ruled out. Viewed in terms of the quantum mechanical WKB (Wentzel-Kramers-Brillouin) approximation, the hard reflection of a wavefunction at a turning point corresponds to a so-called “loss” of phase (phase shift by  $\pi$ ) compared to the soft reflection caused by tunneling (phase shift by  $\pi/2$ ). This shortcoming can be remedied with EBK quantization conditions by addition of a value of  $1/4$ , for each librational turning point, to the corresponding quantum number. Such is the case for the electron’s elliptical and hyperbolic librations in the above quantization, Eq. (19ab), but not for a rotation about the  $z$  axis, Eq. (19c). Strand and Reinhardt call these quantization conditions “primitive” to distinguish them from more sophisticated ones, specified below.

A semiclassical treatment of a free  $H$  atom with EBK quantization has recently been presented in these pages.<sup>19</sup> In this case the isotropic symmetry permits a separation of variables in spherical coordinates,  $r$ ,  $\theta$  and  $\varphi$ , and the EBK quantization conditions are like Eqs. (19abc) except for  $j = r, \theta$ . The atomic ground state is characterized by the quantum numbers  $(n_r, n_\theta, n_\varphi) = (0, 0, 0)$ . Accordingly, the action in the atom’s ground state,  $A_1 = 1h$ , is attributed only to tunneling at the radial and latitudinal turning points (the former being the nucleus). Applying EBK quantization to the ground state of  $H_2^+$ , denoted  $1s\Sigma_g$  in molecular spectroscopy, SR likewise assign the quantum numbers  $(n_\xi, n_\eta, n_\varphi) = (0, 0, 0)$ .

## B. Results

Energies of the Coulomb oscillator (CO), in adiabatic dependence on the proton separation, are listed in Appendix B and shown in Fig. 7 in com-



parison with exact quantum mechanical (QM) results and the semiclassical calculation by SR.<sup>15</sup> The lower part of Fig. 7 shows the electronic energy  $E_{el}(R)$  of the ground state,  $1s\Sigma_g$ . At *large* proton separations,  $R > 6 r_B$ , both the SR calculation (circles) and the CO approach (crosses) agree excellently with the exact QM values (curve). This is the situation where the electron stays near one nucleus (see Fig. 5). As Fig. 7 further shows, such agreement ceases once the classical electron motion leads beyond the molecular bisector, which happens for proton separations below the bifurcation value,  $R < \tilde{R} \approx 5.57 r_B$  (see Fig. 6). Interestingly, the deviations of CO and SR from QM are opposite over the entire range. The SR results are *discontinuous* at a certain proton separation,  $R^* \approx 1.38 r_B$ . Remarkably, at (or near) that value,  $R^*$ , the CO energy crosses the curve of the QM solution.

Adding to the electronic energy  $E_{el}$  the proton-proton repulsion gives the *total* energy  $E$ , Eq. (15). The middle part of Fig. 7 shows by the dashed curve the exact total energy  $E(R)$  of the  $1s\Sigma_g$  ground state, obtained from QM and, by symbols, the corresponding CO and SR values. The solid dot at the minimum of the curve shows the QM equilibrium energy, in agreement with experiment,  $E_0 = -1.20 R_y$ , and the equilibrium internuclear distance,  $R_0 = 2.00 r_B$ . The CO energy ( $\times$ ) comes out too low, due to the inaccuracy of its  $E_{el}$ , with an equilibrium value  $E_0(CO) \approx -1.38 R_y$  at  $R_0(CO) \approx 2.5 r_B$ . Conversely, the SR energy ( $\square$ ) comes out too high with  $E_0(SR) \approx -1.05 R_y$  at  $R_0(SR) \approx 5 r_B$ . Since the CO and SR results deviate about equal and oppositely from QM, their *average* ( $\diamond$ ) is close to the exact values with a minimum of  $E_0[\frac{1}{2}(CO + SR)] \approx -1.19 R_y$  at  $R_0[\frac{1}{2}(CO + SR)] \approx 2.5 r_B$ .

The molecular binding energy is the difference of  $E$  in the molecule and in the constituting atoms, here,  $E_0(H_2^+) - E(H)$ . The energy of a free hydrogen atom,  $E(H) = -1 R_y$ , is indicated in Fig. 7 by the fine horizontal line. Both semiclassical treatments, CO and (barely) SR, yield molecular binding energies with *negative* values and thus a *stable* molecule ion. Why are they more successful than the early attempts, in the 1920s, by Pauli,<sup>4</sup> and independently Niessen,<sup>20</sup> with the Sommerfeld quantization conditions of the old quantum theory?

For the same reason that Sommerfeld had excluded the angular quantum number  $l = 0$  for the  $H$  atom—avoidance of electron collision with the nucleus—both Pauli and Niessen excluded electron motion in the nuclear plane of the  $H_2^+$  molecule ion. They then found the lowest admissible quantum state to be  $(n_\xi, n_\eta, n_\varphi) = (0, 1, 1)$ , denoted  $2p\Pi_u$  in molecular spec-

troscopy, with  $E_0(P, N) = -0.52 R_y$  at  $R_0(P, N) = 5.53 \pm 0.01 r_B$ , depicted by the triangle in the top part of Fig. 7. The QM energy<sup>21</sup> of that quantum state is  $E_0(2p\Pi_u) = -0.27 R_y$  at  $R_0(2p\Pi_u) \approx 8 r_B$ , marked by the solid dot at the minimum of the dotted curve. Since both these energy values are higher than the ground state of a free hydrogen atom, they give rise to *positive* molecular binding energies and thus to spontaneous dissociation,  $H_2^+(2p\Pi_u) \rightarrow H + H^+$ . Qualitatively, Pauli’s and Niessen’s finding of energetic *instability* is borne out by quantum mechanics for this excited state of  $H_2^+$  (Pauli’s argument<sup>4</sup> about “dynamical stability” notwithstanding). The deviation of their historical value ( $\Delta$ ) from the (dotted) QM curve is remarkably small—comparable to those of the CO and SR results for the ground state. Pauli’s and Niessen’s misfortune, though, was that they *misinterpreted* their result as the molecule ion’s ground state—an assessment with fateful consequences in the development of quantum theory.

### C. Discussion

Why do the semiclassical results of the Coulomb oscillator and of SR’s quantization deviate from the QM solution of the  $H_2^+$  molecule ion? Strand and Reinhardt explain the deviation of their primitive quantization from QM with effective potential barriers arising from constrictions due to conservation of both the energy  $E$  and the bifocal Runge-Lenz component  $\Omega_c$  (the angular momentum vanishes for the ground state,  $\mathbf{M} = 0$ ). The most drastic consequence of those barriers is the discontinuity of  $E_{el}$  at  $R^*$  (see Fig. 7) and the large deviations at closer proton separation,  $R < R^*$ . While the simulation of quantum mechanical tunneling beyond the semiclassical turning points of librations is adequately achieved by EKB quantization under the isotropic symmetry of a free  $H$  atom,<sup>19</sup> Eq. (19) is less successful under the lower symmetry of  $H_2^+$ . When SR remedy the situation with “unified” semiclassical quantization conditions, then  $E_{el}$  agrees, for all practical purposes, with QM. Those unified quantization conditions, going well beyond Eq. (19), are sophisticated in their dependence on  $E_{el}$ ,  $\Omega_c$ , and the hyperbolic turning points  $\eta_{\pm}$ . They will not be discussed here.

The reason for the deviation of the CO results from the QM values is the *neglect* of the electron’s *wave* nature in the underlying quantization condition, Eq. (16). In proposing his wave hypothesis de Broglie<sup>22</sup> already showed that the quantization condition of the Bohr model,  $A_n = nh$ , is equivalent

to  $n$  standing waves along the  $n$ th Bohr orbit. If  $s$  denotes the position along the Bohr orbit, then the de Broglie wave can be expressed as  $w(s) = \sin[2\pi a_n(s)/h]$ , with the variable  $a_n(s) = (A_n/S_n) \int_0^s ds'$  along the orbit's circumference  $S_n = 2\pi r_n$ . A generalization gives for the Coulomb oscillator of a free  $H$  atom in the ground state ( $n = 1$ ), its de Broglie wave as

$$w(z) = \sin[2\pi a(z)/h] \quad (20a)$$

with

$$a(z) = m \int_0^z v(z') dz' \quad (20b)$$

and the speed  $v(z')$  from Eq. (2). This de Broglie wave, shown by the line curve in Fig. 8 for a free  $H$  atom positioned at  $+c$ , has a node at the nucleus and at each turning point. By the above characterization, those turning points are “soft,” and it is their softness that ensures the exact energy of the free atom. However, when Eq. (20ab) is applied to  $H_2^+$  for proton separations beyond the bifurcation value,  $R > \check{R}$ , with axial speed from Eq. (8ab) and integration away from the occupied nucleus,  $\int_c^z \dots$ , then the de Broglie wave is found to be “truncated” (no nodes) at both the outer and inner turning point (see Fig. 8, small circles). Those turning points are “hard” and give rise to incorrect energies. Qualitatively, an augmentation of the truncated de Broglie wave with (exponential) “tunneling tails,” determined by the negative kinetic energy in the classically “forbidden” region, would “soften” the turning points. This would give rise to an *effective* far turning point farther out,  $C_{eff} > C$ , and accordingly raise the CO energy, Eq. (7), toward the QM result.

When the proton separation is below bifurcation,  $R < \check{R}$ , then Eq. (20b) should be integrated from the midpoint 0 in both the axial and lateral direction rather than favoring one nucleus with the node of the de Broglie wave. Again, the de Broglie wave is found to be truncated at the axial and lateral turning points,  $C$  and  $B$ , respectively (see Fig. 9). An exception exists for the proton separation  $R^*$ . The de Broglie wave, shown in Fig. 10, then has a minimum at both turning points,  $w(C) = w(B) = -1$ , according to action values of  $A_z = \frac{3}{4}h$  and  $A_y = \frac{1}{4}h$ . Such turning points seem to be “benign”—reminiscent of the soft turning points in the free-atom case—and cause the CO energy  $E_{el}(R^*)$  in Fig. 7 to be *exact*. At still smaller proton separation,  $R < R^*$ , the de Broglie wave is truncated again (not shown). The limit  $R = 0$  corresponds to a Coulomb oscillator in the free  $He^+$  ion which, like in the

free  $H$  atom for  $R = \infty$ , has de Broglie nodes at the turning points and an exact energy value.

If the explanation that the CO energy  $E_{el}(R)$  deviates from the QM curve because of the *neglect of wave effects* is valid, then this sheds new light on the SR results. The opposite sign of the CO and SR deviations then suggests that SR’s primitive EBK quantization, while appropriate for a free atom, simulates *too much wave effects* under the lower symmetry of the  $H_2^+$  molecule ion. However, the *average* of both those semiclassical quantizations seems to be an excellent compromise, as evidenced by the close agreement of the corresponding total energy ( $\diamond$ ) with the (dashed) QM curve in Fig. 7.

In conclusion, semiclassical quantization can rise to Gutzwiller’s challenge and “explain” the chemical bond in the paradigm molecule,<sup>23</sup>  $H_2^+$ , by a combination of classical mechanics, quantization, and moderate wave effects.

## IV. ACKNOWLEDGMENTS

I thank Duane Siemens and Ernst Mohler for valuable discussions. Many thanks to Preston Jones for help with computer integration and graphics. I also thank Professor Gutzwiller for advice and his kind encouragement.

## V. APPENDIX A: QUANTIZATION

By Eq. (4) the action integral of the atomic Coulomb oscillator is

$$A = \frac{1}{\phi} \oint p_z dz = -\frac{4e}{\phi} \sqrt{2Zm} \int_{\Gamma}^0 \sqrt{\frac{1}{z} - \frac{1}{\Gamma}} dz. \quad (4')$$

For a comparison with integral tables we change notation to  $x = z$  and use the abbreviation  $a = -1/\Gamma$ . Then

$$\int \sqrt{\frac{1}{z} - \frac{1}{\Gamma}} dz = \int \sqrt{\frac{1}{x} + ax} dx = \int \frac{\sqrt{X}}{x} dx \quad (21)$$

with  $X = ax^2 + x$ . Integration tables give

$$\int \frac{\sqrt{X}}{x} dx = \sqrt{X} + \frac{1}{2} \int \frac{dx}{\sqrt{X}}. \quad (22)$$

The first term on the rhs, evaluated at the limits of the  $\int_{\Gamma}^0$  integration, vanishes. The last integral in Eq. (22), tabulated as

$$\int \frac{dx}{\sqrt{X}} = (-\sqrt{\Gamma}) \arcsin(1 - 2x/\Gamma), \quad (23)$$

and evaluated at the limits,  $x = 0$  and  $x = \Gamma$ , contributes

$$- [\arcsin(1) - \arcsin(-1)]\sqrt{\Gamma} = -\pi\sqrt{\Gamma}. \quad (24)$$

Combining Eqs. (4'), (22) and (24), together with a fold-out factor  $\phi = 2$ , gives the action integral, to be equated with the Sommerfeld quantization condition,

$$A_n = -\frac{4e}{\phi} \sqrt{2Zm} \frac{1}{2} (-\pi\sqrt{\Gamma}) = nh. \quad (25)$$

We square Eq. (25) and solve for the amplitude of the quantized Coulomb oscillator,

$$\Gamma_n = 2 \frac{r_B}{Z} n^2, \quad (26)$$

in terms of the Bohr radius  $r_B$ .

## VI. APPENDIX B: DATA

TABLE I. Electronic ground-state energy  $E_{el}$  for various nuclear separations  $R$  of the  $H_2^+$  molecule from quantum-mechanical calculations (QM, Ref 21), the “primitive” semiclassical quantization of Strand and Reinhardt (SR, Ref. 15), and the present Coulomb-oscillator approach (CO).

R ( <i>a.u.</i> )	QM ( $R_y$ )	SR ( $R_y$ )	CO ( $R_y$ )
0.00	-4.00	-4.00	-4.00
0.25	-3.80	-4.75	-3.35
0.50	-3.47	-4.27	-3.12
0.75	-3.11	-3.76	-2.93
1.00	-2.90	-3.34	-2.81
1.25	-2.68	-3.07	-2.67
1.50	-2.50	-2.19	-2.55
1.75	-2.34	-2.09	-2.45
2.00	-2.21	-1.99	-2.36
2.50	-1.99	-1.79	-2.18
3.00	-1.82	-1.66	-2.02
3.50	-1.69	-1.56	-1.87
4.00	-1.59	-1.49	-1.75
5.00	-1.45	-1.40	-1.54
6.00	-1.36	-1.33	-1.38
8.00	-1.26	-1.25	-1.27
10.00	-1.20	-1.20	-1.20
12.00	-1.17	-1.17	-1.17

## References

- <sup>1</sup>Other failures were its inability to give the brightness of spectral lines and the unsuccessful extension to the *He* atom.
- <sup>2</sup>M. Jammer, *The Conceptual Development of Quantum Mechanics* (McGraw-Hill, New York, 1966), p. 129.
- <sup>3</sup>Instead of the traditional notation  $k$  for the angular quantum number in the old quantum theory, we will use the letter  $l$  ( $= k$ ) to facilitate the connection with quantum mechanics.
- <sup>4</sup>W. Pauli, “Über das Modell des Wasserstoffmolekülions,” *Annalen der Physik* **68**, 177-240 (1922). A history of Pauli’s thesis is given by C. P. Enz, “No Time to be Brief: A Scientific Biography of Wolfgang Pauli” (Oxford UP, 2002), pp. 63-74.
- <sup>5</sup>M. C. Gutzwiller, *Chaos in Classical and Quantum Mechanics* (Springer, New York, 1990), p. 36.
- <sup>6</sup>A. Sommerfeld, “Zur Quantentheorie der Spektrallinien,” *Annalen der Physik*, **51**, 1-94 (1916).
- <sup>7</sup>This length of semiminor axis has been modified from Sommerfeld’s original expression,  $b_{nl} = (r_B/Z)nk$ , to achieve agreement with expressions from quantum mechanics.
- <sup>8</sup>If the nuclear charge is uniformly distributed, then  $Z'(r) = (r/r_N)^3Z$ , and the electron’s motion inside the nucleus is harmonic.
- <sup>9</sup>M. Bucher, D. Elm and D. P. Siemens, “Average position in Kepler motion,” *Am. J. Phys.* **66**, 929-930 (1998).
- <sup>10</sup>L. Pauling and E. B. Wilson, *Introduction to Quantum Mechanics* (Dover, New York, 1935) p. 144.
- <sup>11</sup>Although almost all quantum texts use the weaker statement “at the nucleus.”
- <sup>12</sup>M. Bucher, “The electron inside the nucleus: An almost classical derivation of isotropic hyperfine interaction,” *Eur. J. Phys.* **21**, 19-22 (2000).

- <sup>13</sup>A. Einstein, “*Zum Quantenansatz von Sommerfeld und Epstein*,” Verh. Dtsch. Phys. Ges. **19**, 82-92 (1917). A summary with modern comments is given by A. D. Stone, “*Einstein’s unknown insight and the problem of quantizing chaos*,” Phys. Today, Aug. 2005, pp. 37-43.
- <sup>14</sup>Eq. (3), introduced as Sommerfeld quantization for familiarity’s sake, is also an Einstein quantization condition.
- <sup>15</sup>M. P. Strand and W. P. Reinhardt, “*Semiclassical quantization of the low lying electronic states of  $H_2^+$* ,” J. Chem. Phys. **70**, 3812-27 (1979).
- <sup>16</sup>The (one-center) Runge-Lenz vector,  $\mathbf{\Omega} = \mathbf{v} \times \mathbf{L} - Ze^2\mathbf{r}/r$ , of a Sommerfeld orbit of angular momentum  $\mathbf{L}$  has a magnitude proportional to the ellipse’s eccentricity  $\varepsilon$  and points from the nucleus toward the perihelion; see J. Morehead, “*Visualizing the extra symmetry of the Kepler problem*,” Am. J. Phys. **73**, 234-239 (2005). For a Coulomb oscillator ( $L = 0$ ,  $\varepsilon = 1$ ),  $\mathbf{\Omega}$  oscillates and thus is *not conserved*. Neither is  $\Omega_c$  of the two-center *Coulomb oscillator* conserved; see H. A. Erikson and E. L. Hill, “*A Note on the one-electron state of diatomic molecules*,” Phys. Rev. **75**, 29-31 (1949); and also C. A. Coulson and A. Joseph, “*A constant of the motion for the two-center Kepler problem*,” Int. J. Quantum Chem. **1**, 337-347 (1967).
- <sup>17</sup>The trajectory will eventually revisit an arbitrarily close neighborhood of any previous point.
- <sup>18</sup>Ref. 5, pp. 207-215.
- <sup>19</sup>L. J. Curtis and D. G. Ellis, “*Use of the Einstein-Brillouin-Keller action quantization*,” Am. J. Phys. **72**, 1521-1523 (2004).
- <sup>20</sup>K. F. Niessen, “*Zur Quantentheorie des Wasserstoffmolekülions*,” Annalen der Physik **70**, 129-134 (1923).
- <sup>21</sup>M. M. Madsen and J. M. Peek, At. Data **2**, 171 (1971); E. Teller and H. L. Sehlin, in *Physical Chemistry, An Advanced Treatise* (Academic, New York, 1970), Vol. **5**, p. 35.
- <sup>22</sup>L. de Broglie, “*Ondes et quanta*,” Comptes Rendus **177**, 507-510 (1923).
- <sup>23</sup>K. Ruedenberg, “*The physical nature of the chemical bond*,” Rev. Mod. Phys. **34**, 326-276 (1962).



## VII. FIGURE CAPTIONS

Fig. 1. Partial trajectory of an extranuclear orbit  $XX'$  and of a penetrating orbit  $PP'$  through nucleus  $N$ . The dotted line  $S$  shows the major symmetry axis of  $XX'$ .

Fig. 2. Line orbit of a Coulomb oscillator with nucleus at origin 0 and turning points at  $\pm\Gamma$ .

Fig. 3. Axial electron speed  $v$  vs. position  $z$  of an electron in Coulomb oscillation for the ground state,  $n = 1$ , of a hydrogen atom  $H$  ( $Z = 1$ , solid curve) and a helium ion  $He^+$  ( $Z = 2$ , dashed curve). The area under one wing of each curve represents the radial action,  $A = 1h$ .

Fig. 4. Axial Coulomb oscillation in an  $H_2^+$  molecule ion between axial turning points  $\pm C$  and through nuclei at  $\pm c$ ; perpendicular oscillation between lateral turning points  $\pm B$  and through midpoint 0.

Fig. 5. Axial speed  $v$  vs. position  $z$  in the ground state of an  $H_2^+$  molecule ion (bold curve) and, for comparison, of a free  $H$  atom (thin curve). Circles indicate the axial the positions of the nuclei, here with a *large* separation,  $R = 6 r_B$ .

Fig. 6. Axial speed  $v$  vs. position  $z$  in the ground state of an  $H_2^+$  molecule ion (M-shaped bold curve) and, for comparison, of a free  $H$  atom ( $\Lambda$ -shaped thin curve, centered at the right nucleus). The  $\cap$ -shaped dotted curve, centered at 0, shows the lateral speed  $u$  vs. the perpendicular position  $y$  in the molecule. Circles indicate the axial positions of the nuclei, here with a *small* separation,  $R = 2 r_B$ .

Fig. 7. Dependence of energies of  $H_2^+$  on internuclear distance  $R$ . *Bottom:* Electronic energy  $E_{el}$  from quantum mechanics (QM, solid curve), primitive semiclassical quantization by Strand and Reinhardt (SR,  $\circ$ ) and the present Coulomb-oscillator approach (CO, +). *Middle:* Total energy  $E$  of the  $1s\Sigma_g$  ground state from QM (dashed curve) with minimum ( $\bullet$ ), values by SR ( $\square$ ) and CO ( $\times$ ) and their average ( $\diamond$ ), energy of a free  $H$  atom (dashed horizontal line). *Top:* Total energy  $E$  of the  $2p\Pi_u$  state from QM (dotted curve) with minimum ( $\bullet$ ), and historical value by Pauli and Niessen ( $\triangle$ ).

Fig. 8. de Broglie wave of the free  $H$  atom Coulomb oscillator (curve) and of the  $H_2^+$  Coulomb oscillator (small circles) for the same proton separation as in Fig. 5,  $R = 6 r_B$ . Large circles indicate the axial positions of the nuclei.

Fig. 9. de Broglie wave of the  $H_2^+$  Coulomb oscillator along axial distance  $OC$  from Fig. 4 (right side of graph) and lateral distance  $OB$  (left side).

Large circles indicate the axial positions of the nuclei, here with the same separation as in Fig. 6,  $R = 2 r_B$ .

Fig. 10. Same as Fig. 9 but for the proton separation  $R^* = 1.38 r_B$  where the semiclassical energy is exact.